Master's thesis

NTNU
Norwegian University of Science and Technology
Faculty of Information Technology and Electrical Engineering
Department of Electric Power Engineering

Abraham Paulsen Sørdalen

Optimal Integration and Control of Distributed Batteries for Multiple Grid Services

Master's thesis in Energy and Environmental Engineering
Supervisor: Jayaprakash Rajasekharan
Co-supervisor: Magnus Korpås
June 2022

NTNU
Norwegian University of Science and Technology

Abraham Paulsen Sørdalen

Optimal Integration and Control of Distributed Batteries for Multiple Grid Services

Master's thesis in Energy and Environmental Engineering
Supervisor: Jayaprakash Rajasekharan
Co-supervisor: Magnus Korpås
June 2022

Norwegian University of Science and Technology
Faculty of Information Technology and Electrical Engineering
Department of Electric Power Engineering

NTNU
Norwegian University of
Science and Technology

Abstract

The electrification of society and the increased power generation from highly variable, intermittent and distributed Renewable Energy Resources (RES) can cause imbalance, instability, and congestions in the transmission- and distribution system. The electricity system requires distributed and smart power flexibility. A promising means for such flexibility is Battery Energy Storage Systems (BESS). BESS can provide multiple power flexibility services to all stakeholders in the electricity system; the power producers, the power consumers and "pro-sumers", the Distribution System Operators (DSO), and the Transmission System Operators (TSO). Typically, BESS have been deployed for only one or two flexibility services. In this thesis, however, a concept is developed for BESS to provide multiple services to several of the stakeholders. Moreover, the concept integrates and controls a fleet of distributed units to achieve the desired temporal and spatial flexibility.

The work includes the development of a modular system model for distributed batteries and an agent-based control concept. The hierarchical, agent-based control system provides energy arbitrage, peak-shaving, and reserve market services. The distributed agents derive BESS service scheduling based on their consumption forecasting and various statistical analysis. A Central Controller (CC) is included to act as an aggregator and market maker between the agents. The CC enables the individual BESS agents to trade services between themselves. Through a rescheduling of services, the distributed BESS can jointly enhance the provision of total power response to the electricity system and increase the operational profitability. In addition to the development and analysis of the modular model and control concept, a Python-based simulator has been developed. The analyses show that the proposed concept with the distributed agent-based BESS enables each BESS to provide multiple grid services. Moreover, it is shown that the cooperation via a central coordinator enables each BESS to re-prioritise between local flexibility needs and regional flexibility needs based on updated forecasting. The proposed distributed agent-based BESS concept optimises hence the support for both temporal imbalances between total generation and consumption of electricity, as well as for spatial congestions in the grid. As an example, the proposed concept enables a battery system to decide when it should be used for providing more power to an overloaded transformer or EV charging station, or when to generate revenues from reserve markets to stabilize the frequency of the grid.

Sammendrag

Med elektrifiseringen av samfunnet og økt kraftproduksjon fra svært variable, intermitterende og distribuerte fornybare energiressurser kan forårsake ubalanse, ustabilitet og overbelastninger i transmissions- og distribusjonssystemet. Elektrisitetssystemet trenger distribuert og smart kraftfleksibilitet. Et lovende middel for slik fleksibilitet er batterisystemer. Batterisystemer kan tilby flere strømfleksibilitetstjenester til alle interessenter i elektrisitetssystemet; kraftprodusentene, kraftforbrukerne og «pro-sumers», distribusjonssystemoperatørene, og transmisjonssystemoperatørene. Vanligvis har batterisystemer blitt brukt for bare én eller to fleksibilitetstjenester. I denne oppgaven er det imidlertid utviklet et konsept for at batterisystemer skal levere flere tjenester til flere av interessentene. Dessuten integrerer og kontrollerer konseptet en flåte av distribuerte enheter for å oppnå ønsket fleksibilitet.

Arbeidet omfatter utvikling av en modulær systemmodell for distribuerte batterier og et agentbasert kontrollkonsept. Det hierarkiske, agentbaserte kontrollsystemet gir energiarbitrage, peak-shaving og reservemarkedstjenester. De distribuerte agentene utleder tjenesteplanlegging basert på deres forbruksprognoser og ulike statistiske analyser. En sentral kontroller er inkludert for at batteri-agentene skal handle tjenester seg imellom. Gjennom en omlegging av tjenester kan de distribuerte batterisystemene i fellesskap øke leveringen av total effektrespons til elektrisitetssystemet og øke lønnsomheten. I tillegg til utvikling og analyse av den modulære modellen og kontrollkonseptet, er det utviklet en Python-basert simulator. Analysene viser at det foreslåtte konseptet med den distribuerte agentbaserte BESS gjør at hvert batterisystem kan tilby flere nettjenester. Videre vises det at samarbeidet via en sentral koordinator gjør at hvert batterisystem kan omprioriteres mellom lokale fleksibilitetsbehov og regionale fleksibilitetsbehov basert på oppdaterte prognoser. Det foreslåtte distribuerte agentbaserte-konseptet optimerer derfor støtten for både tidsmessige ubalanser mellom total produksjon og forbruk av elektrisitet, så vel som for overbelastninger i nettet. Som et eksempel lar det foreslåtte konseptet et batterisystem bestemme når det skal brukes til å gi mer strøm til en overbelastet transformator eller el-ladestasjon, eller når det skal generere inntekter fra reservemarkeder for å stabilisere frekvensen til nettet.

Preface

This thesis is written as a part of the TET4900 - Electric Power Engineering and Smart Grids coarse at NTNU, spring 2022. The master thesis is a continuation of the specialization report written in fall 2021 [1].

I would like to thank my supervisor, Associate Professor Jayaprakash Rajasekharan, for his insight and inspiration during this thesis. I would like to thank my co-supervisor, Professor Magnus Korpås, for constructive feedback and help with the thesis. I would also like to thank Ole Jakob Sørdalen at Pixii AS and Lede AS for providing power consumption data and for providing valuable insights.

Contents

Abstract . . . **iii**
Sammendrag . . . **iv**
Preface . . . **v**
Contents . . . **vi**
Figures . . . **ix**
Tables . . . **x**
Abbreviations . . . **xi**
1 Introduction . . . **1**
1.1 Background . . . 1
1.2 Motivation . . . 2
1.3 Research question . . . 2
1.4 Contribution of the thesis . . . 3
1.5 Thesis outline . . . 3
2 Literature Review . . . **5**
2.1 Energy- and ancillary services from BESS . . . 5
2.1.1 Energy arbitrage . . . 6
2.1.2 Peak-shaving . . . 6
2.1.3 Frequency control and reserve markets . . . 7
2.1.4 Battery degradation as a factor in operation cost . . . 7
2.2 Power consumption forecasting . . . 7
2.3 Optimization and control . . . 8
2.4 Multi-Agent based energy management . . . 10
3 Theory . . . **11**
3.1 Battery Energy Storage Systems (BESS) . . . 11
3.1.1 Flexibility . . . 11
3.1.2 Battery degradation as a factor in operation costs . . . 12
3.2 Power consumption forecasting . . . 12
3.2.1 Long Short Term Memory . . . 13
3.2.2 Facebook Prophet . . . 14
3.3 Peak-shaving and energy arbitrage . . . 14
3.3.1 Monthly maximum power tariff . . . 14
3.4 Reserve markets . . . 17
3.4.1 Frequency Containment Reserves - FCR . . . 17
3.4.2 Fast Frequency Reserves - FFR . . . 17

3.4.3 Bidding on the reserve markets . . . 18
3.5 Optimization and control . . . 19
4 Methodology . . . 22
4.1 Background . . . 22
4.2 Battery integration for grid service participation . . . 25
4.3 Grid services . . . 26
4.4 Data usage . . . 26
4.5 Assumptions . . . 28
4.5.1 Battery assumption . . . 28
4.5.2 Market assumptions . . . 28
4.6 Model description . . . 29
4.7 Prophet consumption forecasting . . . 30
4.8 Optimization . . . 32
4.8.1 Stage 1 optimization: Job scheduling . . . 33
4.8.2 Stage 2 optimization: SOC planning . . . 36
4.8.3 Stage 3 optimization: Agent job rescheduling and trading . . 39
4.9 Simulation interface . . . 42
4.9.1 Subplot 1: Market prices . . . 43
4.9.2 Subplot 2: Job schedule and power consumption forecast . . 43
4.9.3 Subplot 3: SOC planning . . . 44
4.9.4 Subplot 4: Local market trading . . . 44
4.10 Simulation scenarios . . . 44
4.10.1 Base case . . . 45
4.10.2 Scenario 1: Additional large consumers . . . 45
4.10.3 Scenario 2: C-rating change . . . 45
4.10.4 Scenario 3: FFR removed . . . 45
4.10.5 Scenario 4: 2021 energy prices . . . 45
5 Results . . . 47
5.1 Prophet consumption forecasting . . . 47
5.2 Optimization . . . 49
5.2.1 Peak-shaving optimization . . . 49
5.2.2 Cost of flexibility . . . 51
5.3 Scenario presentation description . . . 52
5.4 Base case . . . 55
5.5 Scenario 1: Additional large consumers . . . 56
5.6 Scenario 2: C-rating change . . . 57
5.7 Scenario 3: FFR removed . . . 58
5.8 Scenario 4: 2021 energy prices . . . 59
6 Discussion . . . 60
6.1 Results discussion . . . 60
6.1.1 Prophet forecasting . . . 60
6.1.2 Base case . . . 61
6.1.3 Scenario 1: Additional large consumers . . . 63
6.1.4 Scenario 2: C-rating change . . . 63

6.1.5 Scenario 3: FFR removed 64
6.1.6 Scenario 4: 2021 energy prices 64
6.2 Model performance 64
6.2.1 Optimization 64
7 Conclusion and future work 66
Bibliography 68

Figures

3.1 Categories of machine learning forecasting methods 12
3.2 LSTM time-step cell structure. Figure inspired by [34]. 14
3.3 Peak-shaving with capacity step bounds 16
3.4 Bidding and market clearing times for energy- and reserve markets. 19

4.1 Simplistic battery and agent flow chart. 23
4.2 Communication link between battery agents. 24
4.3 Battery integration with consumer and grid operators. 25
4.4 Model flowchart. 29
4.5 48 hour Prophet forecast, commercial building 1. 30
4.6 Forecast deviation with Gaussian function, commercial building 1. . 32
4.7 Optimization stages. 33
4.8 Minimum SOC allocation for peak-shaving and energy arbitrage service optimization using consumption forecast and prediction interval. 37
4.9 SOC planning for energy arbitrage service optimization with minimum SOC constraints. 38
4.10 1 hour forecast improvement using Autoregression for local market service trading. 40
4.11 Supply and demand market clearing process. 41
4.12 Simulation GUI for commercial building 1. 43

5.1 Forecast deviation from actual values, Commercial building 1. . . . 48
5.2 Forecast deviation from actual values, Commercial building 2. . . . 48
5.3 Flexibility cost from cheapest to most expensive. 52

Tables

2.1 BESS application services [4]. 6

3.1 Prices with monthly maximum power tariff at Lede AS [38] 15
3.2 Reserve markets bidding restrictions 18
3.3 Conventional and intelligent search optimization methods [44] . . . 21

4.1 Data used and their sources. 27
4.2 Total probability [%] of consumption being under each capacity step for the entire month, commercial building 1 and 2. 35

5.1 MAPE, MAE and MSE of 10 consumers using the Prophet algorithm. 47
5.2 Probability [%] of consumption being under each capacity step for 10 time steps, commercial building 2. 49
5.3 Total probability [%] of consumption being under each capacity step for an entire month, commercial building 1 and 2. 50
5.4 Reserve market bid compared to consumption forecast and under 50kW capacity level probability for 10 hours, commercial building 1. 50
5.5 Reserve market bid compared to consumption forecast and under 50kW capacity level probability for 10 hours, commercial building 2. 50

Abbreviations

ACO	Ant Colony Optimization
aFRR	automatic Frequency Restoration Reserve
BESS	Battery Energy Storage Systems
BMS	Battery Management System
CC	Central Controller
CCS	Centralized Control System
CNN	Convolutional Neural Networks
CNP	Contract Net Protocol
DAM	Day-Ahead-Market
DBS	DC-Bus Signaling
DCL	Digital Communication Link
DER	Distributed Energy Resources
DG	Distributed Generation
DOD	Depth Of Discharge
DSO	Distribution System Operator
EFR	Enhanced Frequency Response
EMD	Empirical Mode Decomposition
FCR	Frequency Containment Reserves
FCR-D	Frequency Containment Reserves for Disturbances
FCR-N	Frequency Containment Reserves for Normal operation
FFR	Fast Frequency Reserves

FL	Fuzzy Logic
GA	Genetic Algorithm
GAM	Generalized Additive Model
HS	Harmony Search
KDE	Kernel Density Estimator
LP	Linear Programming
LSTM	Long Short-Term Memory
MAPE	Mean Absolute Percentage Error
MAPSO	Multi-Agent Particle Swarm Optimization
MAS	Multi-Agent System
MILP	Mixed-Integer Linear Programming
MINLP	Mixed Integer Non-Linear Programming
NLP	Non-Linear Programming
OPF	Optimal power flow
pdfs	probability density functions
PEV	Plug-in Electric Vehicles
PSO	Particle Swarm Optimization
PV	Photovoltaic
RES	Renewable Energy Resources
RKOM	Regulatory power options market
RNN	Recurrent Neural Network
SOC	State Of Charge
SVR	Support Vector Regression
TSO	Transmission System Operator
XGBoost	Extreme Gradient Boosting

Chapter 1

Introduction

1.1 Background

Political and social discourse is becoming increasingly environmentally oriented. The EU aims to reduce greenhouse emissions by 55% within 2030 and achieve climate neutrality by 2050 [2]. Significant investments towards emission intensive sectors are being made by governments to reduce pollution. The production of electrical energy is CO2 intensive has therefore been targeted with governmental incentives for an energy transition towards Renewable Energy Sources (RES). Advancements in technology has improved the cost-effectiveness of solar and wind utilization. Solar photovoltaic (PV) and wind power generation costs have seen a downward trend in recent years, increasing RES utilization investments. Recent geopolitical developments in Europe has reiterated the need for energy independence and the need for having an economy less exposed to fossil fuel supply chain issues. A large issue with PV and wind power generation is the intermittency of production and low inertia. Intermittent power generation can cause discrepancies in the generation and consumption balance. A low inertia power system offers low resistance when disturbances are introduced and can in a worst case scenario cause continental blackouts. Ancillary reserve markets have been implemented by the Transmission System Operator (TSO) to acquire sufficient reserve power capacity.

The Electrical Vehicle (EV) penetration in Norway is the highest in the world per capita [2]. 54% of all new cars sold are electric, resulting in a total 12% of the car park being electric. Without incentives, consumers tend to charge EV's during peak consumption hours. This causes congestion risks in parts of the distribution systems that is not designed for large loads. Distribution System Operators (DSO) in Norway have planned to create incentives to consumers to reduce peak power consumption by implementing a monthly maximum power tariff that rewards low consumption peaks.

The implementation of BESS into grid operations has become increasingly cost effective with the reduction of BESS costs. Battery systems provide flexibility at a rapid pace compared to traditional flexibility providers. The analysis of battery systems in grid utilization is therefore worth exploring.

1.2 Motivation

There are dangers that persist in the power system. The power system is susceptible to harsh weather, frequency disturbances, geopolitical events, congestion, continent wide blackouts, and much more. Many problems in a modernised power grid can be solved with fast and reactive systems, and with good communication and control. Battery systems can provide society with energy security and reliability when implemented right. With the flexibility of battery systems, multiple grid services could be provided at different time slots or at the same time. The digitalization and automation of battery systems can help society create a robust and efficient electricity system. The research of BESS in grid utilization could therefore contribute to societal changes that ultimately increases social welfare.

When considering the practicality and feasibility of a technical solution, it is important to examine the socioeconomic values of society. The value of the technical solution is directly related to the social or economic value it can provide society. Businesses in western capitalist countries are constantly working to cut costs and increase profits. Therefore, creating a technical solution that serves the interests of a business could provide the business with good investment opportunities.

The challenge of providing multiple grid services is the planning and scheduling of services that the battery system can provide when subjected to stochastic and unpredictable data. The energy- and flexibility markets are structured to require participation bids many hours or days ahead of the activation time. This causes challenges for BESS that need to predict the values of the services ahead of time using stochastic data. Agent-based modelling is a promising field of study that give battery systems the ability to communicate and trade market obligations. This could relieve the battery system of the burden of participating in the wrong service if the forecast deviates.

1.3 Research question

The master thesis aims to answer the following research questions:

- Can a control model be implemented for distributed BESS to provide multiple grid services?
    - Which grid services can distributed BESS provide?
    - How can agent-based modeling be utilized to control BESS?

To answer the research question, the master thesis aims to:

- Identify relevant services that BESS can provide, and the market driven economic incentives.
- Study the characteristics of energy arbitrage, peak-shaving and reserve market participation services and research the constraints in the FFR-, FCR-, energy markets and the utility tariffs that are relevant for these applications.
- Research power consumption forecasting and optimization methods to determine service priority for distributed BESS.
- Develop a model that acts as a proof of concept for the feasibility of distributed BESS providing multiple grid services. Implement the Prophet forecasting algorithm and utilize forecasts to optimize service allocation 48 hour ahead. Create a central control system that performs market clearing and promotes agent cooperation to increase flexibility.
- Evaluate the flexibility of the proposed model on several scenarios and determine the operational feasibility of the implemented model.

1.4 Contribution of the thesis

In this thesis a model was developed that demonstrated the feasibility of providing multiple grid services using distributed battery systems. The model acts as a proof of concept and gives insights into potential commercial applications. The model gives insight into how grid service participation can be implemented into a modular and scalable system, and how varying battery and market characteristics change the service prioritization and revenue streams.

The thesis contributes with a method of implementing agent based programming in the power system. The model proved the ability of agents to cooperate to increase system flexibility and revenue. The model also utilizes the stochasticity of power consumption to solve optimization problems connected to service scheduling.

The most important contributions of the thesis is the creation of a model that:

- Demonstrates the feasibility of BESS providing multiple grid services.
- Demonstrates that agent-based modelling can be used to increase BESS cooperation, flexibility and revenue.

1.5 Thesis outline

The master thesis is a continuation of a specialisation report written in the fall of 2021 [1]. Therefore, several sections are taken from the specialisation report. Especially Chapter 2 and 3 is inspired by the specialization report [1]. The literature review chapter is found in Chapter 2. The literature review gives historical and theoretical insight into previous work on the thesis subject. Chapter 3 includes theory on important and relevant concepts to give the theoretical background for the thesis. The model implementation and design is presented in Chapter 4. The results from the model are presented in Chapter 5. The discussion of the thesis is found in Chapter 6. Finally, the conclusion and future work is presented in Chapter 7.

Chapter 2

Literature Review

A thorough literature review is necessary to give insight into relevant research topics for this master thesis. The literature review will therefore analyze previous research of how BESS can provide consumers and the power grid with essential services. Previous work on standardized integration with and without agent-based modeling techniques is important to analyze the relevance and efficiency of different optimization solutions. The literature presented in this chapter gives insight into different aspects of the project objective, and it is therefore important to critically assess the work to be able to apply the best solutions to this thesis.

2.1 Energy- and ancillary services from BESS

There is an increase in popularity towards utility-scale BESS due to instantaneous ramping, short response time and the operational flexibility [3]. A study of BESS applications by [4] found possible utilization services given in table 2.1.

The siting and sizing of distributed storage systems is important to optimize the cost-effectiveness of a BESS when providing the services mentioned in table 2.1. [5] proposes a three-stage method of determining near-optimal siting and sizing of the distributed storage systems. The method uses Mixed-Integer Linear Programming (MILP) to determine unknown variables in segmented stages. In this thesis the siting of the BESS are assumed to be optimal to focus on specific services: energy arbitrage, peak-shaving and frequency support.

Integrating BESS with unpredictable renewable energy sources has operational advantages. The Tehachapi wind energy storage project [6] installed 8MW/32MWh with 13 specified operational uses, including energy arbitrage and frequency regulation. The area in which the BESS is installed is known to have insufficient transmission capacity, resulting in wind curtailment contingencies. The BESS aims to reduce the probability of wind curtailment by discharging when wind power output is more than 80% in preparation of a contingency. In normal operation, the BESS will charge and discharge based on a periodic dispatch profile.

Table 2.1: BESS application services [4].

Applications	Description
Congestion support	Reduce load and generation peaks.
Voltage support	Ensure power quality.
Frequency support	Ensure balance between production and consumption by participation in reserve markets.
Loss minimization	Control power flow to reduce losses in distribution grid.
Redundancy	Increase power system redundancy. Provides backup power redundancy.
Energy arbitrage	Purchase power at cheap prices and sell at expensive prices. Could also increase self-consumption of local production.
Peak-shaving	Reduce power-based utility tariff costs by reducing peak consumption.

2.1.1 Energy arbitrage

A useful application of BESS is energy arbitrage. The Battery Management System (BMS) can exploit the energy price fluctuations in the power market to buy power in periods when energy is cheap and sell when energy is expensive. This is also known as time of use optimization. Comprehensive studies have been performed to optimize energy arbitrage on the power market during periods with volatile changes in power prices. [7] tested an energy arbitrage model with PV on power markets in New York, Ontario and Queensland. The results showed that revenue and profitability was highly dependant by high variations in energy prices and the volatility. [8] proposed a method of time domain arbitrage opportunities for grid level battery storage in the Day-Ahead-Market (DAM) with the possibility of corrections in the real-time-market. The research found that longer lasting batteries generate lower profits due to the longer time it takes to charge/discharge when considering investment costs.

The research conducted in [7] and [8] explored the feasibility of energy arbitrage and energy storage, but excluded discussions regarding combining energy arbitrage with other services. The lack of feasibility performing energy arbitrage as the primary service has been thoroughly researched. BESS allow for quick response time and provide the grid with unique capabilities and flexibility. Energy arbitrage should therefore act as a supplementary service and not a primary service.

2.1.2 Peak-shaving

Peak-shaving is an important service to prevent congestion on the distribution grid. [9] developed a peak-shaving method with integrated feed-in PV power and

BESS. The method deployed a regression-based Box Jenkins forecasting algorithm to determine when the battery would need to shave the feed-in PV power. Regardless of a high Mean Absolute Percentage Error (MAPE) of almost 39%, the algorithm managed to perform peak-shaving. The strategy of peak-shaving feed-in PV power can be combined with reducing peak load, while also increasing self-consumption.

2.1.3 Frequency control and reserve markets

The Nordic power system has several reserve markets to ensure that the balance of production and consumption is at all time balanced. [10] proposed a model where 75% of the revenue is from the energy market and 25% is from the reserve market. [11] proposed a control algorithm to provide the UK transmission network operator with Enhanced Frequency Response (EFR), which is the faster frequency response service in the UK.

Adding a constraint on the revenue share between the energy- and reserve market as was done in [10] can reduce total revenue and is not optimal.

2.1.4 Battery degradation as a factor in operation cost

Battery degradation is an important factor in investment analysis and in calculating operation costs. [5] has assumed that the operating cost of battery cycling is negligible and assumes a fixed lifespan of 20 years. This assumption is not valid since frequent cycling expedites the degradation of battery cells [12]. Battery degradation dependencies are complex and difficult to model. To reduce complexity, [3] made the following assumptions:

- The effect of ambient temperature is neglected.
- The effect of charge/discharge rate is neglected.
- The maximum and minimum limits of State Of Charge (SOC) results in the degradation effect of deep and shallow charging/discharging being neglected.
- The rate of degradation is equal when charging and discharging.

[13] reduces degradation in distributed battery systems in a microgrid by either charging or discharging all the batteries at a given time. This reduces circulating currents and thus, degradation.

2.2 Power consumption forecasting

For a system with distributed battery systems with multiple functions it is important to develop a model that forecasts power consumption. Research on forecasting time-series stochastic data presents strategical variations. Different applications require higher accuracy on either short-term and long-term forecasting. The probability density functions (pdfs) of prices in [8] and [14] are determined using a quantile-copula Kernel Density Estimator (KDE). [15] analyses the accuracy of the Prophet algorithm and how it compares to the ARIMA algorithm. The Prophet algorithm uses factors like season, time, weather and electricity price in the prediction model and [15] claims it has better accuracy than the ARIMA algorithm in consumption prediction. The Prophet algorithm provides an estimation method that incorporates long-term time variant trends, but is not entirely reliable in predicting the short-term variations in power consumption. [16] developed a hybrid model consisting of Convolutional Neural Networks (CNN) and M-BDLSTM which outperformed CNN, Long Short-Term Memory (LSTM) and integrated CNN-LSTM models. The model trained using 60 minutes of historical data to forecast the next 60 minutes with a one-minute sampling rate. LSTM requires greater computational power, but also has a greater ability of learning from long-term sequence dependencies than CNN. [17] proposed a decomposition accumulation principle combined with Empirical Mode Decomposition (EMD) and Extreme Gradient Boosting (XGBoost) algorithm to forecast month ahead consumption using hourly data points. The EMD-XGBoost algorithm was tested on seven years with data and outperformed conventional forecasting methods in most forecasted months. [18] proposed a Support Vector Regression (SVR), multiple load forecasting method based on particle swarm optimization. The model forecasted 15 minutes using one month as test data. SVR is a robust, supervised, regression-based forecasting method that focuses on risk minimization. [18] found that the SVR based forecasting method was better suited to minimizing structural risk than traditional neural networks.

Applied methods of sequential stochastic data forecasting researched in [15] and [17] is long-term and the emphasis on accurate data forecasting succeeding the cut-off period is not a priority. Forecasting methods researched in [14], [8], [18] and [16] provide short-term predictions, and are optimized to analyze short-term data trends, but do not account for seasonal and weekly consumption trends. XGBoost uses a lookback period to indicate correlation between data, meaning that XGBoost is highly dependent on seasonal trends. The forecasting accuracy is significantly reduced if consumption data is volatile and unpredictable compared to short-term regression-based methods. Despite the proposed model presented in [17] outperforming the conventional forecasting methods, there was one month where the model underperformed compared to the other methods. This represents a weakness in the implemented model.

2.3 Optimization and control

Effective optimization and control strategies for distributed BESSs are vital to provide necessary services. [19] identified three communicative control principles for microgrids; decentralized control, centralized control and distributed control.

While the stabilization obligations of a islanded microgrid are fundamentally different than grid-connected DERs, the communication strategies are transferable. The traditional, decentralized control strategy, DC-Bus Signaling (DBS), was used in a hybrid renewable nanogrid [20]. With DBS the units operate independently and a failure in a node will not inherently hinder functionality. The case study presented integrated wind power, PV, a diesel generator and a battery bank. The simulations showed the feasibility of the DBS to schedule storage and nonrenewable backup generation in a DC nanogrid. [21] proposed a hierarchical, four-layer, centralized control architecture for a grid-connected, hybrid microgrid. The four layers in the hierachical structure are: local controllers of power electronics, coordination of components for optimized power distribution, grid synchronization/power flow/stability, and data analysis on system status. The proposed control system performed optimal power sharing. [22] proposed a multiagent based distributed control model to minimize operation costs of a microgrid. The communication links were established between direct neighbors of the distributed generation agents and simulation results confirmed a reduced operational cost.

The research presented in [20], [21] and [22] is conducted in the framework of micro- or nanogrids. Decentralized-, centralized, and distributed control in microgrids are viable solutions, but the weaknesses with the control strategies become more prevalent in systems needing scalability, operational security and low computational complexity as is explained in section 3.5. A hybrid approach between the strategies can mitigate the challenges.

The proposed optimization method in [23] utilizes a mixed integer linear programming (MILP) problem for the power market in Ontario, USA, to maximize revenue in a cryogenic energy storage system (CESS) using the day-ahead/week-ahead and real-time electricity markets. A scenario-based stochastic model with a linear quantity-only bidding model and a MILP price-quantity bidding model was developed in [8]. The model is useful to determine price scenarios in the DAM and the Real-Time Market (RTM). The model does not incorporate battery degradation as a result of battery cycling, SOC and Depth Of Discharge (DOD) as a constraint in the optimization problem. Battery degradation affects the lifetime of the battery system and is therefore an important consideration when maximizing profits. Robust optimization is a variant of traditional LP and MILP, and typically employs an uncertainty set that includes the worst-case scenarios [24]. Robust optimization has been used in [25] and has proven to yield better results when processing uncertain power prices than deterministic approaches.

The optimization of power arbitrage in [19]-[22] does not consider the possibility of participating in other ancillary services or markets. This undermines the flexibility and potential provided by battery systems. Linear programming techniques are computationally efficient but are constrained to not allow nonlinear effects. Linearization of nonlinear effects are therefore necessary to reduce computational complexity.

2.4 Multi-Agent based energy management

Major advantages with multi-agent systems is the ability to distribute computational burden to local agents which can optimize the decision making process for the individual entity. [26] attributed agents to individual energy producers, storage units and loads to ensure sufficient energy supply in a microgrid. The agents communicate with a microgrid central controller using Contract Net Protocol (CNP). In the CNP procedure the agents acquire data from the central controller. The agents use artificial intelligent algorithms to determine the bids that would maximize benefits for the agent/entity. The central controller then activates the cheapest production units to satisfy the demand. If there is insufficient aggregated power available, the central controller will either force generation or perform load-shedding. [27] uses a strategy of Multi-Agent Particle Swarm Optimization (MAPSO) for power flow in large scale distributed BESS. The proposed model is designed to control the power flow and keep the SOC of each BESS at a proper level. Simulations on data from a wind power station was used to validate the method. MAPSO can be useful to solve non-linear optimization problems but does not necessarily find the optimal solution.

[27] and [26] have used energy flow models, meaning the models are based on techno-economic analysis and power flow balance. [13] implements a dynamic model, which focuses on the power electronics as well as the power flow. [13] presents a non-linear sliding mode control model for SOC balancing in a microgrid with distributed battery systems. The model ensures that all the batteries are either charging or discharging to remove circulating currents and reducing degradation. Whilst the primary control is a standard V-I droop control used for decentralized load sharing, the secondary control level regulates the average BESS output voltage and ensures accurate current sharing between the BESSs.

Processing stochastic data has embedded randomness and there are therefore control systems in need of agents with capabilities of making decisions in systems with uncertainty. [26] and [28] uses fuzzy logic with "degrees of truth" rather than boolean logic in their artificial intelligence algorithms to determine when to charge/discharge based on the SOC and to protect the battery against deep discharge. The method is useful to establish a probability of the agent performing a certain action.

Cooperation between agents is important to increase flexibility and profitability. Using a Bayesian Nash Equilibrium game-theoretic based bidding strategy has been researched in [29]. The agents used information about other demand response aggregators to create bids to maximize personal profits.

Chapter 3

Theory

The theory being presented in this chapter will act as supporting material for the model presented in chapter 4.

3.1 Battery Energy Storage Systems (BESS)

Increased distributed stationary storage can be valuable to help alleviate challenges that occur when integrating Plug-in Electric Vehicles (PEV) and RES [4]. BESS can be a cost effective alternative to building new transmission lines or increasing transformer capacity. There are several technical difficulties that arise with DER as described in Chapter 3. Batteries can help solve some of the challenges by providing voltage support, producing/consuming reactive power and improving power quality. The characteristics of BESS allow it to participate in ancillary services, energy markets and reserve markets. The battery can act as a generator or load depending on the SOC [24].

Round trip efficiency is an important metric in determination of charge/discharge scheduling and energy arbitrage. Round trip efficiency is the percentage of stored energy that can later be retrieved. The higher round trip efficiency, the less energy loss in the storage process. Tesla Powerwall 2, which is a battery system used for commercial applications with a rated 5kW/14kWh, has a specified 90% round trip efficiency [30].

3.1.1 Flexibility

A key term in power systems is "flexibility". The definition of flexibility in power systems varies depending on the specific part of the power system being discussed and the literature [31]. In the context of this project, flexibility is the ability of the battery system to provide the services through market price signals. The stakeholders in the electricity system has the ability to indirectly activate services provided by the battery system by increasing the asking price in the relevant market. The battery system will therefore provide the stakeholders with operational flexibility. The relevant price signals sent by the DSO is the utility tariff, which can be adjusted over time if peak demand is not substantially reduced. The relevant price signals sent by the DSO are the reserve market prices.

3.1.2 Battery degradation as a factor in operation costs

Minimizing operational costs is an important factor when making market bids that reflect the marginal operating cost of the BESS [10]. The rate of battery degradation is dependant of several factors[3].

- DOD
- Charge and discharge rate
- Ambient temperature
- Battery maintenance procedures

For this thesis, these factors are not a factor in an optimization problem. Degradation is reflected in the total lifetime of the battery system, which is assumed to be 12 years. [32] finds a minimum of 22% and maximum of 80% DoD to be the optimum bounds to minimize lifetime cost and life cycle CO_2 emissions.

3.2 Power consumption forecasting

Time series forecasting has been a vital part of business planning in a modern and competitive environment. Forecasting is therefore widely researched in statistics, econometrics, time series analysis and in machine learning applications. This thesis will only research some of the previously discussed forecasting methods. The forecasting models discussed in section 2.2 represent different categories of statistical analysis and machine learning. Figure 3.1 describes the subcategories in machine learning that the forecasting models fall under.

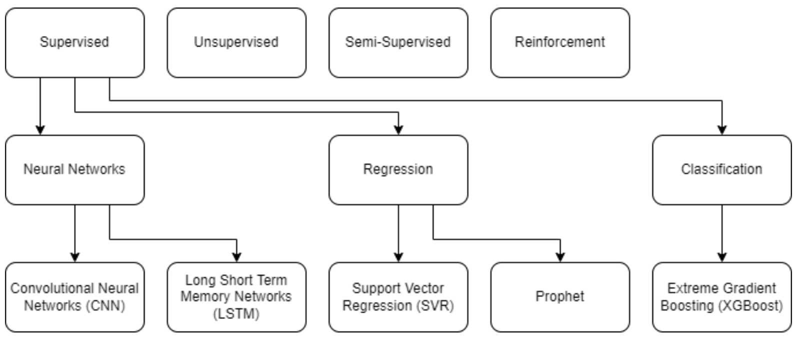

Figure 3.1: Categories of machine learning forecasting methods

There are advantages and disadvantages with each forecasting method, and a deeper understanding of the underlying properties of the forecasting methods is necessary to get an accurate short-term and long-term prediction. The properties of LSTM and Facebook Prophet are discussed in the subsequent sections.

3.2.1 Long Short Term Memory

LSTM is researched in this thesis, but is ultimately not used in the developed model presented in Chapter 4 due to sub-optimal results from the developed LSTM model.

LSTM was proposed in 1997 by Hochreiter and Schmidhuber[33]. LSTM is used in the field of deep learning and uses a Recurrent Neural Network (RNN) structure [34][35]. LSTM is designed to be accurate with both short-term and long-term sequential time-series problems. Information is memorized through cell states, input gate sigmoid functions, forget gates, output gates and add sum operation with tanh function to reduce the probability of gradient disappearance and explosion [35]. LSTM aims to solve the vanishing gradient problem that the traditional RNN method suffers from. The gradient is the parameter used to update a neural networks weight. RNN is not as computationally complex as the evolved LSTM, but suffers from a diminishing gradient when the gradient backpropagates through time, thus leading to short-term memory. The structure of the cells in the LSTM model is presented in figure 3.2 where the red circles indicate a sigmoid function and the blue circles indicate a tanh-function. The cell takes in information of the input information, the previous hidden state and the previous cell state. The forget gate decides which input data should be kept and which should be forgotten. The information passes through a sigmoid function that gives the data a value between 1 (keep) and 0 (forget). The closer the data is to 1, the more likely the information will be kept. The input gate is the regulatory gate that creates a new cell state. The output state decides the hidden state that should be carried over to the next time-step. LSTM is a comprehensive and widely used forecasting strategy that produces viable results in power consumption forecasting [35]. Due to LSTM being more computationally complex than traditional RNN, the frequency of forecasting needs to be evaluated.

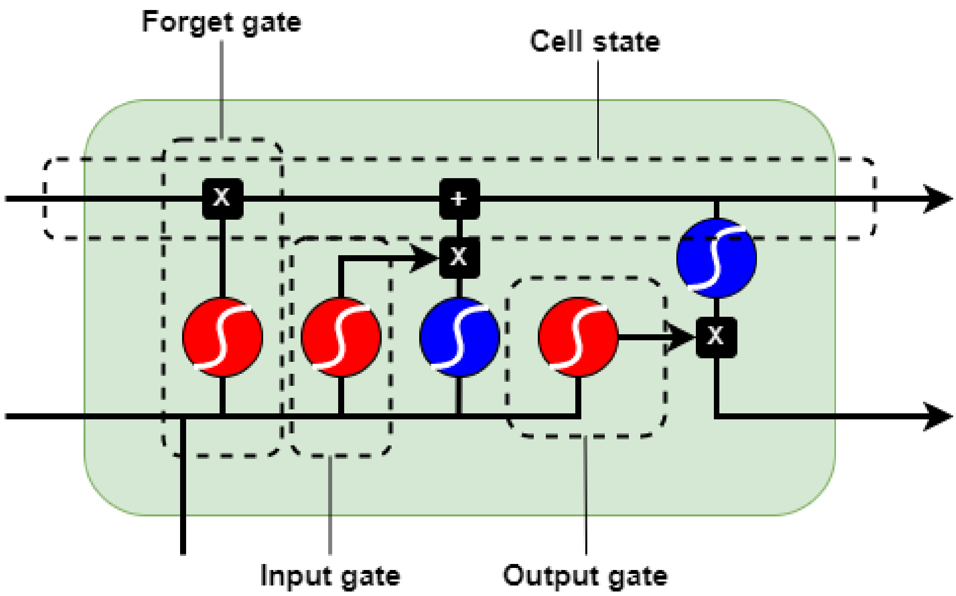

Figure 3.2: LSTM time-step cell structure. Figure inspired by [34].

3.2.2 Facebook Prophet

Prophet is a forecasting model designed by Facebook to primarily forecast sales and business expectations [36]. The model is designed with adjustable parameters that allow for human tuning. Prophet has three main model components; trend, seasonality and holidays. The model also encompasses an error term, ϵ_t, which is assumed to be normally distributed. The specifications of the Prophet model is similar to the Generalized Additive Model (GAM) from 1987 [37]. The Prophet model uses time as a regressor with the possibility of using several linear and non-linear functions of time as components. The model incorporates trend changes by automatically defining changepoints, which can also be manually specified by an analyst for incoming catalysts. Though Prophet successfully observes trends, the method lacks in the ability to predict short-term outcomes after the cutoff period. The model is meant for data with clear and quantifiable trends. Power consumption on a per-user-basis can be volatile and unpredictable, and consumption can therefore have a large discrepancy compared to the overall trend. The preliminary results in section 5.1 of the Prophet forecasting method show the model creating a prediction based on hourly consumption, season and trend.

3.3 Peak-shaving and energy arbitrage

3.3.1 Monthly maximum power tariff

In the context of BESS, peak-shaving refers to actively reducing demand by injecting battery stored power into the distribution system in periods with high power demand from the user. The DSO will get a lower reading from the electricity meter than they would have received without peak-shaving. The opposite is true when the BESS is charging. The observed consumption will be higher. Using BESS to peak-shave is presently a useful service for large scale businesses that have a power-based utility tariff and for DSOs that wish to reduce grid expansion costs. A large portion of electricity costs are charged by the DSO for the grid services provided. Distribution lines have a maximum capacity limit, and it is therefore important for the DSO to either contain peak power distribution within the bounds or upgrade the distribution capacity. Large consumers therefore have a maximum power tariff to incentivize lowering the maximum peak demand. Peak-shaving as a service has an economic directly for the consumer and indirectly for the DSO. In 2022 several DSOs in Norway are planning to implement a maximum power utility tariff for households. The utility invoice will consist of a fixed cost and an energy cost. The fixed cost will be decided by which step the maximum hourly power consumption during a month falls under in table 3.1. For most households the fixed price increases every 5kW interval.

Capacity step	**Price including VAT (kr/month)**
0-5 kW	266.25
5-10 kW	478.75
10-15 kW	691.25
15-20 kW	905.00
20-25 kW	1117.50
25-50 kW	1755.00
50-75 kW	2818.75
75-100 kW	3882.50
100-150 kW	5477.50
150-200 kW	7605.00
200- kW	10795.00
Energy fee	**Price including VAT (kr/kWh)**
Energy winter (nov-mar)	0.16
Reduction night (22:00-06:00)	-0.08
Energy summer (apr-oct)	0.135
Reduction night (22:00-06:00)	-0.0675
Public taxes	**Price including VAT (kr/kWh)**
Energy tax (jan-mar)	0.1114
Energy tax (apr-des)	0.1926
Energifond tax	0.0125

Table 3.1: Prices with monthly maximum power tariff at Lede AS [38]

A well functioning BESS can predict the maximum consumption during a month and will inject power to keep the net consumption within a certain capacity step [9]. Currently businesses with over 100,000kWh yearly consumption get charged

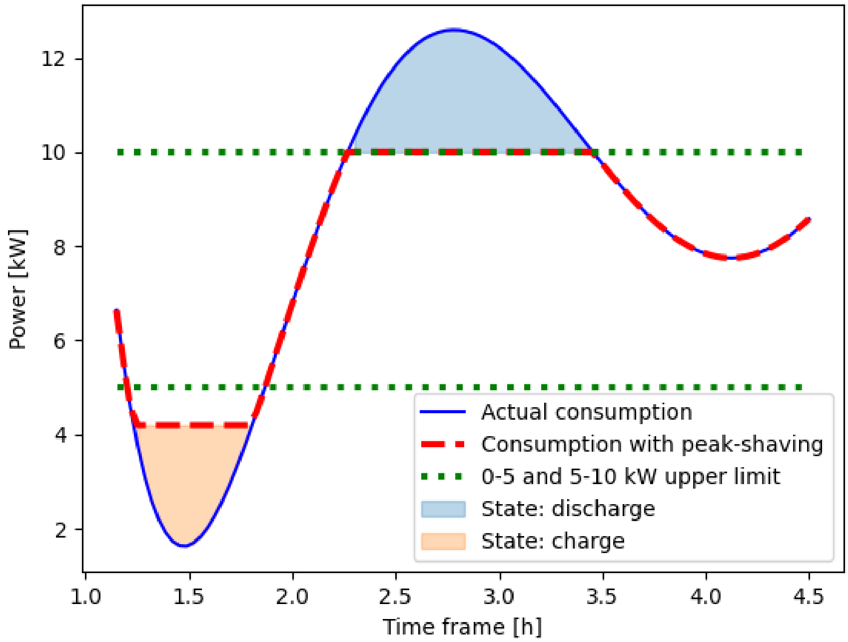

Figure 3.3: Peak-shaving with capacity step bounds

a rate for the highest consumption peak in kr/kW/month [39]. Given the volatile and stochastic nature of power consumption, timing peak consumption is difficult. BESS control systems risk miscalculating the peak, causing the BESS to either discharge when the consumption is close to the peak or discharging too early and depleting the stored energy before the consumption peak has reduced. With 5kW steps, the control system needs to predict which step the consumption will fall under and try to restrict consumption beneath the upper bound of that step. Figure 3.3 represents the control mechanism restricting consumption within the 10kW upper limit. If the control system succeeds in restricting consumption at 10kW for the entire month, the fixed price will be 478.75kr as is shown in table 3.1. Charging of the battery cells is performed when consumption is low and energy prices are low to utilize energy arbitrage. Energy arbitrage utilizes varying energy prices through the day to charge when prices are low and discharge when energy prices are high. Energy arbitrage is a vital part of the optimization problem to maximize profits. Energy arbitrage and peak shaving services often work in tandem to minimize losses and maximize profits.

The ability of the BESS to keep the consumption under 10kW in figure 3.3 is dependant on the power and energy characteristics being sufficient. A battery with power and energy characteristics of 3kW/6kWh can reduce the peak by maximum 3kW and the integral under the power curve above 10kW can maximum be 6kWh.

3.4 Reserve markets

Statnett is the transmission system operator of the Norwegian power system. Statnett is responsible for the balance between production and consumption, which can be observed in the system frequency. The power system is continuously subjected disturbances that may interfere with the power balance [40]. To ensure stable operations Statnett has created primary, secondary and tertiary power reserves that are acquired through markets. The price is determined by the highest accepted bid (Pay as Clear) and the volume of accepted bids is determined by agreed goals set by the TSO regarding frequency quality levels.

3.4.1 Frequency Containment Reserves - FCR

The FCR market acquires the primary reserves needed to stabilize system frequency. The activation of the reserves is entirely automatic. The market is separated into reserves for normal operation (FCR-N) and reserves for operational disturbances (FCR-D). For this thesis, only the FCR-D will be relevant, so for now on when FCR is mentioned it is referring to FCR-D. The FCR market is split into two time slots. The FCR D-2 market acquires reserves two days ahead of activation. The FCR D-1 market acquires reserves one day ahead of activation. The accepted reserve power is automatically activated when there is a ±0.1Hz deviation from the ideal 50Hz [41].

FCR D-1 bids need to be sent before 18:00 the day prior to the bid reservation. FCR D-2 bids need to be sent before 17:30 two days in advance of the bid reservation. The time at which the prices are published is not specified in the guidelines for the FCR markets. It is therefore assumed for this project that participants in the FCR markets get informed on the closing price an hour after bids have been submitted, as is the practice for the FFR markets.

The FCR D-2 market has only been active since the start of 2021. The power consumption data in this master thesis dates back to 2019. To make a worthy simulation on future market conditions the model will create fictitious FCR D-2 market prices dating back to 2019. Since the FCR D-2 prices closely follow the FCR D-1 prices in 2021, the model will create FCR D-2 prices that are proportionally dependant on the FCR D-1 prices. The average FCR D-2 price is found to be 1.59 larger than the average FCR D-1 price for 2021. The FCR D-2 prices for 2019-2020 will therefore be 1.59 larger than the corresponding FCR D-1 prices.

3.4.2 Fast Frequency Reserves - FFR

The fast frequency reserves market is intended for fast activation in scenarios with large power system failures that cause a frequency drop to bellow 49.0 Hz. The main source of electric power in Norway comes from hydro installations [42].

Hydroelectric production provides the power system with high inertia, making the power system resistant to power failures. Hydro reserves are being preserved during the nights in the summer due to low energy prices. In the summer, international power imports and wind energy cover a larger portion of the energy demand, leaving the power system with low inertia and thus, vulnerable to disturbances.

The FFR market has not been fully developed, but a demonstration of the market was run in 2021 with a total of 119MW power was reserved in the needed hours. The FFR market was reserved for hours between 22:00 and 07:00 in the days between 3. May and 3. October. There were two categories in the demonstration of the market, "FFR Profil" and "FFR Flex". The market categories decided the flexibility of the market participants. The decided closing prices of the markets were 11.13 and 49.19 £/MW/h [43]. For this project the FFR market will simulate normal market conditions, where the closing price will be an average between the two mentioned category prices of 30.19 £/MW/h. This will be the fixed price between the hours of 22:00 and 07:00 in the days from 3. May and 3. October. All other hours the price will be 0 £/MW/h.

To simulate an active market, the bid times for this market will be assumed to be the same as the FCR D-1 market and bids will need to be sent at 18:00 the day prior to the bid reservation. The information on the market closing price for the subsequent day will be received at 19:00, an hour after bids have been sent.

3.4.3 Bidding on the reserve markets

Table 3.2: Reserve markets bidding restrictions

Reserve market	Bid time	Bid acceptance time
FCR-N, D-1	18:00	19:00
FCR-N, D-2	17:30	18:30
FFR	18:00	19:00

The FCR-N market demands a minimum bidding volume of 1MW and that the bidding volume is rounded. 1MW, 2MW and 5MW are valid volumes in the bidding process. 1.4MW is not a valid bidding volume. Statnett allows for distributed systems to aggregated the bid volumes and provide one total bid to the specific market. The bidding times on the different markets can be summed up in Figure 3.4.

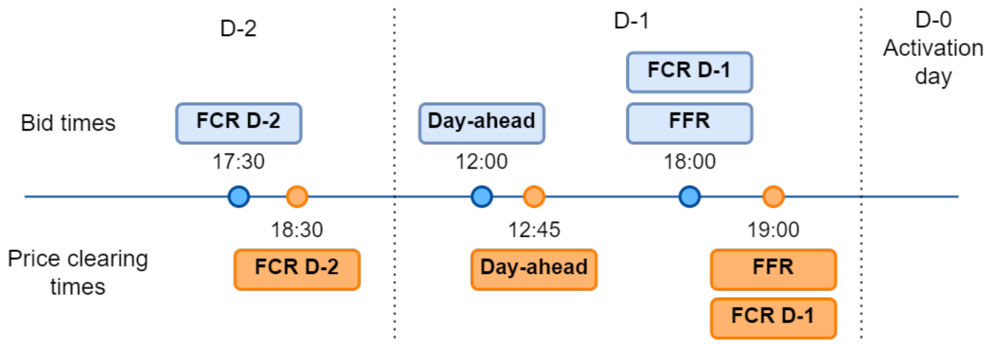

Figure 3.4: Bidding and market clearing times for energy- and reserve markets.

3.5 Optimization and control

There are three main communication strategies deployed on microgrids and with distributed batteries [19].

- Decentralized control - communication links do not exist and power lines is the only mode of communication.
- Centralized control - distributed batteries send data to a centralized aggregator via a digital communication link. The data is processed and feedback commands are sent back.
- Distributed control - digital communication links are implemented between units and control strategies are processed locally.

Decentralized control gives units independent and local control [20]. Decentralized control provide operational security since the units are independent from other units. It also mitigates cyber security risks since control signals are processed locally without connection to a central controller. Decentralized control removes the possibility of communication between units which reduces the ability to cooperate and therefore reduces system flexibility. Centralized control utilizes a central controller that processes all relevant information and provides all the units with control signals. This strategy gives the central controller full overview and therefore the ability to provide the grid with optimal power dispatch. The main challenges with centralized control is the lack of scalability and security. In centralized control each distributed unit has unknown variables that need to be decided with an optimization formulation. When the power dispatch of one unit is dependant on the unknown variables of all the other units, expanding the system with more units can create a large computational burden for the central controller. Centralized control is dependant on the central controller always being functional and connected to each unit. A fault in the central controller can cause a system-wide failure. Distributed control is a control principle with no central controller and the units only communicate amongst themselves through dedicated Digital Communication Links (DCLs) [19]. Distributed control allows for full functionality in the case of a node failure. This control strategy allows for direct cooperation between distributed units, which greatly increases system flexibility. A challenge in distributed control is the increased complexity when expanding the network with more units (nodes). An increase in the number of units, increases the number of DCLs exponentially. There are also technological difficulties creating DCLs between units. The units need data transmission capabilities to establish a DCL. The unit could connect via the internet or with a transmitter with substantial bandwidth and amplification.

Optimization of the operating system is determined by what the objective function is, the constraints on the system, the accuracy of forecasting and the efficiency in agent cooperation. [44] reviewed literature on the optimization techniques that have been used for integration of Distributed Generation (DG) from RES. The methods were divided into conventional methods and intelligent search methods. Artificial intelligence and heuristic methods are considered intelligent search methods. Heuristic methods consist of algorithms that speed up the process of finding near optimal solutions. Heuristic methods are simplistic, but lack accuracy and precision[44]. A brief overview of existing optimization methods is presented in table 3.3.

Conventional opt. methods	**Description**
Linear Programming (LP)	Solve a mathematical problem with linear requirements for maximizing or minimizing the objective function.
Non-Linear Programming (NLP)	Solve a mathematical problem with non-linear requirements for maximizing or minimizing the objective function.
Mixed Integer Linear Programming (MILP)	LP but some variables are discrete and some are continuous.
Mixed Integer Non-Linear Programming (MINLP)	NLP but some variables are discrete and some are continuous. Very difficult to solve.
Optimal power flow (OPF)	Finds optimum economic operating cost while considering the impact of the transmission and distribution system.
Fuzzy Logic (FL)	Rejecting Boolean values (0 or 1) and allocating a value between 0 and 1, modelling uncertainty and indicating level of association of each component.
Intelligent search methods	**Description**
Genetic Algorithm (GA)	Maximizes "fitness" based on principles of natural selection and genetics.
Tabu Search (TS)	Finds the solution space while using adaptive memory and responsive exploration.
Particle Swarm Optimization (PSO)	Particles are created that evaluate and share their fitness level neighboring particles to iteratively acquire the optimal solution. Possibility of only finding local minima
Ant Colony Optimization (ACO)	Particles share their path towards the optimal solution, initialized by random solutions.
Harmony Search (HS)	Optimization based on music theory on achieving better harmony

Table 3.3: Conventional and intelligent search optimization methods [44]

Chapter 4

Methodology

The method chapter in this thesis gives a detailed explanation of a Python developed control model to be implemented in distributed battery systems to provide multiple grid services. An explanation of the background and integration of BESS in grid operations is provided to give validity to the developed model. The use of BESS in grid operations is not a new phenomenon, but as the energy system becomes more renewable and market driven, the possibility of increasing profits and flexibility become apparent. The model developed in this thesis therefore acts as a proof of concept. The concept being that increasing profitability of BESS in grid operations is not only possible, but is a viable strategy to increasing revenue and cutting costs, whilst also increasing the services provided to society.

4.1 Background

In the model developed there are owners of battery systems which will provide the business, the DSO and the TSO with services. The model is designed to maximize economic gains and minimize cost to the owners of the battery systems. This is why the developed model will be using agent based modeling. Each battery system has allocated an agent which acts as the brain of the battery system. The agent is designed to work in the self interest of the battery owners. The agent will also work in the self interest of the battery owners by indirectly cooperating with other agents through a central controller to further increase profits. A simplistic flow chart of the relationship between the battery systems, agents, central controller and the public markets is shown in Figure 4.1.

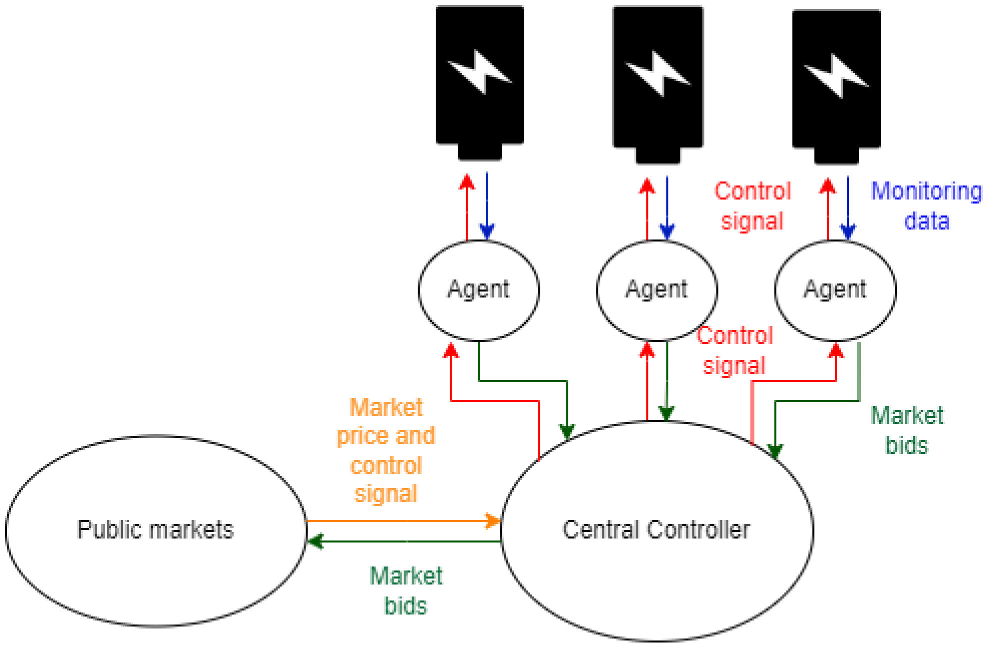

Figure 4.1: Simplistic battery and agent flow chart.

Essentially, the agents will make the decision on how the battery should be utilized. The central controller is designed to be a communication hub between the agents through market mechanisms. While there is a central controller, the communication between the agents happens in a distributed way. The central controller helps facilitate the communication between the agents and the central controller does not make decisions on behalf of any agent. The batteries are therefore distributed, but only needs one digital communication link, which is between an agent and the central controller. This is an important aspect in the model. This design establishes individuality for battery owners while also being scalable. The distributed communication design used in this model is shown in Figure 4.2.

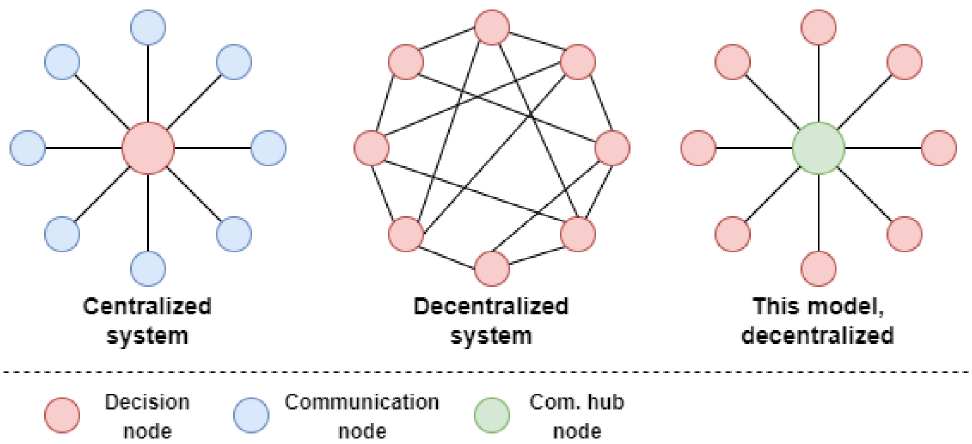

Figure 4.2: Communication link between battery agents.

The communication design in this model employ different aspects of a centralized and decentralized design. The blue nodes indicate an agent that simply collects data but does not process it or make decisions. The red nodes indicate an agent that processes data and makes decision. The green node is a communication hub, where the agents can cooperate without establishing a direct DCL.

The agents in this model make decisions locally. This allows them to optimize their decision making without outside influence. A disconnection of the communication link to the central controller still allows the agent to make control decisions for the battery, but without the capability of cooperating with other agents. Traditional centralized systems lose all operational capabilities on a node if it loses connection to the central controller. The communication design in this model is also considering the increasing need for better cyber security solutions. When the decision making and data processing happens locally, it is difficult for an infiltration into the entire system. Hacking one agent provides information on only that agent. Hacking the central controller provides the information that is being transferred through the digital communication links. In Section 4.8.3 it will become apparent that the information that is being transferred through the DCL's are bids, which is difficult to decrypt into useful information. The major advantage of not using a traditional decentralized communication system is that traditional decentralized communication systems establish many DCL's, which could become computational heavy and makes the model less scalable. The design in this model allows for scalability since an increase in the number of agents increases the total computational time linearly instead of exponentially.

4.2 Battery integration for grid service participation

To get an understanding of how the battery system can perform multiple grid services it is important that the battery system is integrated correctly into the power system. The battery system will be integrated with a consumer behind the electric power meter. This will allow the battery to manipulate the observed power consumption by the DSO by injecting power or charging power using the battery. Pixii AS uses battery systems for implementation in buildings and businesses. The energy rating on their battery systems are calculated to be approximately 25% of the consumers maximum consumption. Their battery systems also have a C-rating 0.5, meaning that the power rating will be 12.5% of the historically maximum consumption of the business or building. The same principle will be used in this thesis. The battery system is therefore sized according to the size of the consumption. A consumer with large power consumption will have a large battery. A consumer with a small amount of power consumption will have a small battery. Figure 4.3 presents the relationship between the consumer, the battery system, the distribution grid and the transmission grid.

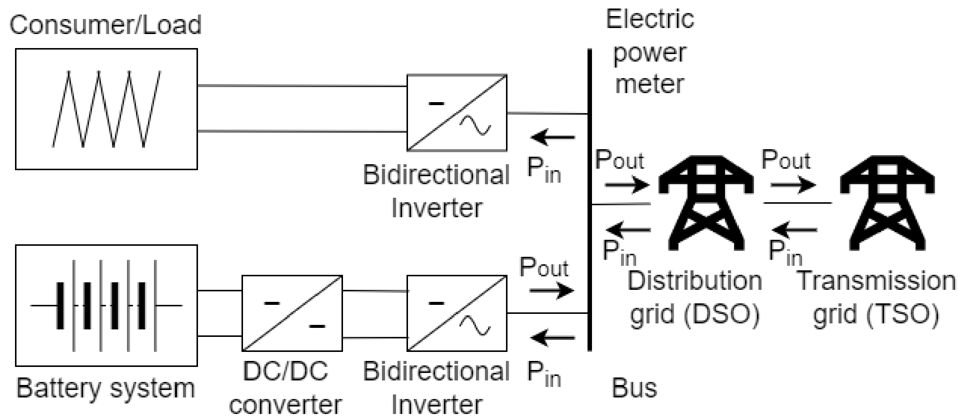

Figure 4.3: Battery integration with consumer and grid operators.

The DSO is the operator for the distribution grid and the TSO is the operator for the transmission grid. Using this relationship the observed power registered by the DSO is calculated using Equation 4.1.

$$P_t^{observed} = P_t^{load} - P_t^{battery} \tag{4.1}$$

When the battery discharges, the observed load by the DSO becomes lower. When the battery charges, the observed load by the DSO becomes higher.

4.3 Grid services

As established in Section 2.1, there are many services BESS can provide the energy system. For this thesis, the battery systems will provide three services; Energy arbitrage, peak-shaving and reserve market participation. These three services have direct economic value since they are either market based or have direct costs attributed to them. It is therefore possible to quantify a value to providing these services.

- Energy arbitrage - The battery system will buy energy in the day ahead market when the price is cheap and sell energy when the energy is expensive. This creates a revenue stream for the battery owner.
- Peak-shaving - Reduce power tariff costs by reducing the observed load. Using the battery system to injecting power during periods where the battery owner has high consumption could reduce the observed load. Reducing the observed load could reduce the power tariff costs imposed by the DSO in conjuncture with the costs in Table 3.1. If the battery system assists the battery owner in reducing the maximum observable load to a lower capacity step, the monthly power tariff costs are reduced.
- Reserve market participation - Participate in reserve market (FCR D-1, FCR D-2 and FFR) bidding to supply the TSO with backup power reserves.

While the model is designed to increase the profitability for the battery owners, the battery system provides increased value to society when providing multiple services. Energy arbitrage helps stabilize prices, such that the price difference between on-peak and off-peak hours are lower. Peak-shaving helps reduce peak demand in the distribution system, which could help the DSO reduce grid investments to combat power congestion. Reserve market participation helps the TSO stabilize the power balance, which helps reduce the probability of a blackout event in the power grid. The incentives to provide these services are both economical but also to improve the operational flexibility of the power system. Both the energy arbitrage and reserve market participation is directly market driven. The agents can bid capacity on the different markets in conjunctions with the rules and regulations described in Section 3.4 and 3.3. The peak-shaving services reduces the monthly utility tariff, so the value of the services is analysed by looking at what the utility tariff would be with or without the battery system.

4.4 Data usage

Developing a model for distributed BESS for multiple grid services requires data. The data will be used to backtest the model to simulate real world applications. The data consists of power consumption data for different users with different consumption characteristics, and market data. The consumption data is hourly consumption data and the duration of the data varies between 1-3 years, between the start of 2019 and end of 2021. The data that is be used to develop and test the model are shown in Table 4.1.

Base case, Consumption data	**Source**	**Avg. consumption [kW]**
Commercial building 1	Pixii AS	35.3
Commercial building 2	Pixii AS	27.4
Aggregated area 1-50	Lede AS	15-60
Scenario 1, Consumption data	**Source**	**Avg. consumption [kW]**
Factory	Pixii AS	3667
Condominium	Pixii AS	114.9
Store 1	Pixii AS	261.4
Store 2	Pixii AS	279.1
Market data	**Source**	**Avg. market price**
Day ahead energy price	Nord Pool	38.7 EUR/MWh
FCR D-1 price	Statnett	6.6 EUR/MW
FCR D-2 price	Statnett	10.5 EUR/MW
FFR price	Statnett	8.2 EUR/MW
Utility tariff	**Source**	
Power tariff table	Lede AS	Table 3.1

Table 4.1: Data used and their sources.

The consumption data for Scenario 1 will be added to the simulation data set when running a specific scenario. This is explained more in detail in Section 4.10.2.

All consumption data provided in this thesis is anonymous. The consumption data from Lede AS is a data set of 960 households. Since this thesis is analysing the use of battery systems in medium scale consumers, the consumption from the households have been aggregated in groups of 20. This is to simulate a condominium or a collective investment. The consumption data for the households were structured geographically, so the aggregated households are geographically close. Testing the model with these aggregated consumers is useful for DSO's since using battery systems in certain geographic areas is becoming increasingly relevant when trying to peak-shave the load of the aggregated consumers instead of increasing grid investments. When considering the aggregated areas as individual consumers, there are in total 50 consumers. There are therefore 50 individual agents in the model.

The model is designed to address the needs of different consumers with different consumption patterns. With the relevant data, the battery system could be connected to an overloaded transformers or EV charging stations. The battery system would provide peak-shaving services when power consumption is high and provide reserve market participation when power consumption is low.

4.5 Assumptions

A theoretical model needs to make several assumptions. Assumptions have to be made to simplify the model without reducing the integrity of the results.

4.5.1 Battery assumption

- The battery energy rating in kWh is 25% of the historical hourly maximum power consumption for the specific agent.
- The battery power rating in kW is 12.5% of the historical hourly maximum power demand for the specific agent.
- The SOC is always between 20% and 80% in support of the optimal operational range found in [32].
- Battery degradation is not a factor in energy cycling calculations. Battery degradation is instead a factor of time, where the total lifetime of operation is assumed to be 12 years.
- The round trip efficiency of the batteries is 90%.
- The base case C-rating is 0.5. A C-rating of 0.5 means that the battery energy storage rating (kWh) is twice as large as the battery power rating (kW).

4.5.2 Market assumptions

- The future market prices are known. The prediction of market prices are outside the scope of this thesis.
- Activation in the reserve markets are rare and are short in duration. A minimum of 20% SOC is sufficient to always participate in the reserve markets.
- The agents or central controller can trade energy instantaneously on the day-ahead market. This can realistically be achieved through agreements with other energy providers that have large bids already approved by Nordpool.
- The bids on the reserve market are not necessarily a minimum of 1MW, as Statnett requires.
- Bids on the reserve market all happen at midnight the day before activation, or two days ahead for the FCR D-2 market.
- The volume of the bids on the markets are not sufficiently large enough to move the price when clearing.
- The TSO allows the battery system to charge and discharge energy irrespective of reserve market participation. If the battery systems is activated in the reserve markets, the battery system will discharge at maximum power capacity.

4.6 Model description

This section describes the model flowchart presented in Figure 4.1 in more detail. A flowchart illustration the main components and the technical and commercial signals is shown in Figure 4.4.

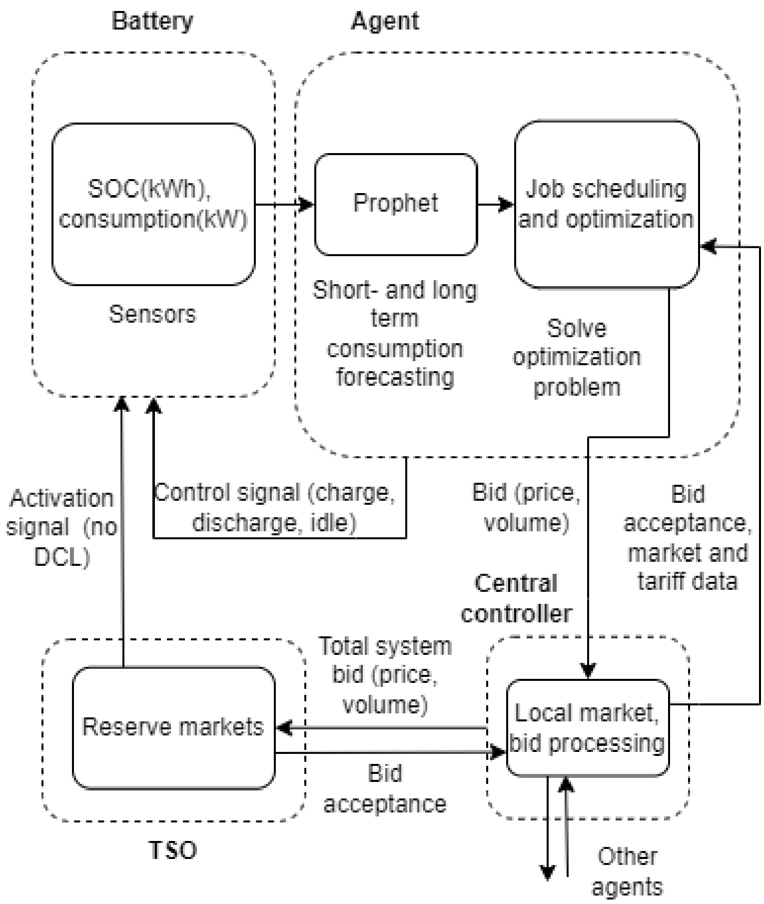

Figure 4.4: Model flowchart.

The model is divided into four segments. The battery segment collects consumption from the battery owner and SOC data from the battery. The agent segment performs forecasting, job scheduling and optimization. It is in the agent segment where most of the calculations and optimization is done. It is in the central controller segment where agents can communicate with each other by trading services and obligations.

4.7 Prophet consumption forecasting

The background and theory to the Facebook Prophet forecasting algorithm is presented in Section 3.2.2. To adhere to the requirements by the reserve markets and day ahead market, the bids to participate on the markets have to be sent a specific time prior to the activation day as shown in Figure 3.4. The model therefore needs to perform job scheduling (service scheduling) in the optimization process. To find the value of each service, the model needs to perform consumption forecasting. The forecast is especially important to determine when the battery system needs to perform peak-shaving services by injecting power and reducing the observable load.

The Prophet algorithm is a versatile forecasting tool with plug and play capabilities. The Prophet forecasting algorithm is attuned to highly time-dependent and seasonal data, which consumption data often is. For the peak-shaving services it is more relevant to know the probability of the consumption surpassing a certain capacity step, because surpassing the capacity step would result in a higher monthly utility tariff. Since consumption data is stochastic, finding the characteristics of the forecasting deviation gives valuable insight into the consumption characteristics. The deviation is determined using a probability input and the characteristics of the historic consumption patterns. The probability is used in the optimization problem to determine if the BESS should provide peak-shaving services. Figure 4.5 shows an example of a 48 hour forecast.

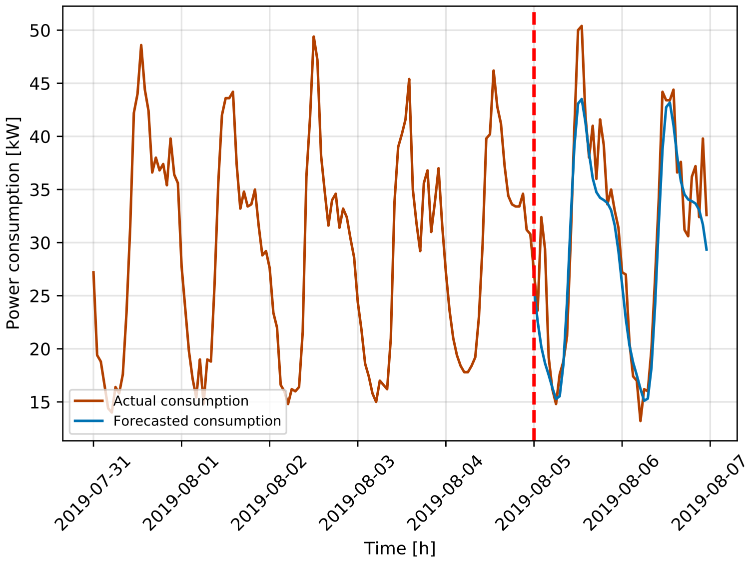

Figure 4.5: 48 hour Prophet forecast, commercial building 1.

The Prophet algorithm does not directly provide the capability of calculating the probability of each forecasted data point being under a certain value. A possible approach to calculate the probability is to assume that the deviation between the forecasted values and the actual values has historically had a Gaussian distribution. Using statistical analysis, the probabilities of exceeding a capacity step can be found for each consumption data point. The Prophet algorithm provides expected forecasted values, $\hat{y}$, and the upper expected deviation values, $\bar{y}$, given a 95% accuracy. 95% is equivalent to a z-score of 1.96. Equation 4.3 shows the relationship between the variables.

$$\sigma_i = \frac{\bar{y}_i - \hat{y}_i}{Z_i} \tag{4.2}$$

where Z_i is the z-score of 1.96. When the standard deviation, σ_i, is calculated, a new z-score can be calculated using the maximum capacity step that the consumption should be under.

$$Z_{i,new} = \frac{\bar{x} - y_i}{\sigma_i} \tag{4.3}$$

where $\bar{x}$ is the maximum power level. The new z-score is converted into a probability score using a Python dictionary that provides a standard normal table. Performing this process for each forecasted hour provides a series of probabilities for the consumption surpassing one of the maximum power levels. This process assumes that the forecasting error is normally distributed. A normally distributed forecasting error is unrealistic for many load profiles. The stochastic characteristics in power consumption can cause large power consumption spikes that are difficult to predict. The forecast could therefore have a high number of larger errors that cause the errors to not follow a normal distribution. The randomness of power consumption is reduced when aggregating over a larger area but the reduction is not significant enough to justify using the above method. Using the historical forecasts and actual values, a proposed method is to map out the percentage forecasted error compared with the actual values. Mapping the error with 1% increments provides the error distribution. An example of the error distribution with the Gaussian distribution function is shown in Figure 4.6.

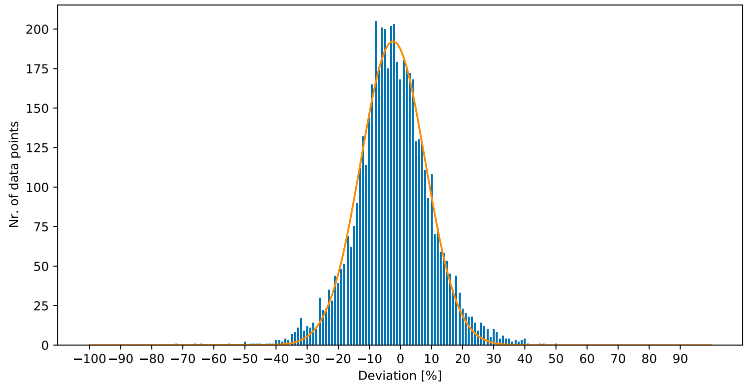

Figure 4.6: Forecast deviation with Gaussian function, commercial building 1.

Using the method of determining probability of exceeding a capacity level using the error deviation is not completely accurate for each data point. The consumption forecast can be overdamped or underdamped, which can lead to the forecast missing predictions in periods where the consumption rapidly increases or decreases. The rapid consumption swings are typically trend correlated and therefore occur at certain hours of the day.

4.8 Optimization

The optimization of multiple battery systems for multiple grid services is inherently complex and has a large number of dependant variables. In computational complexity theory, the optimization problem in this thesis to maximize revenue and minimize costs follows the NP classification (nondeterministic polynomial time), since the set of problems can be solved in polynomial time by a nondeterministic Turing machine. The stochastic nature of energy consumption and market pricing makes an optimal solution in an optimization problem impossible, but this model will utilize statistical analysis to create a good approximation to the optimal solution.

The objective with the optimization is to maximizing revenue and minimize costs. The decision on the service the battery will provide each hour is pertinent to maximizing revenue and minimizing costs.

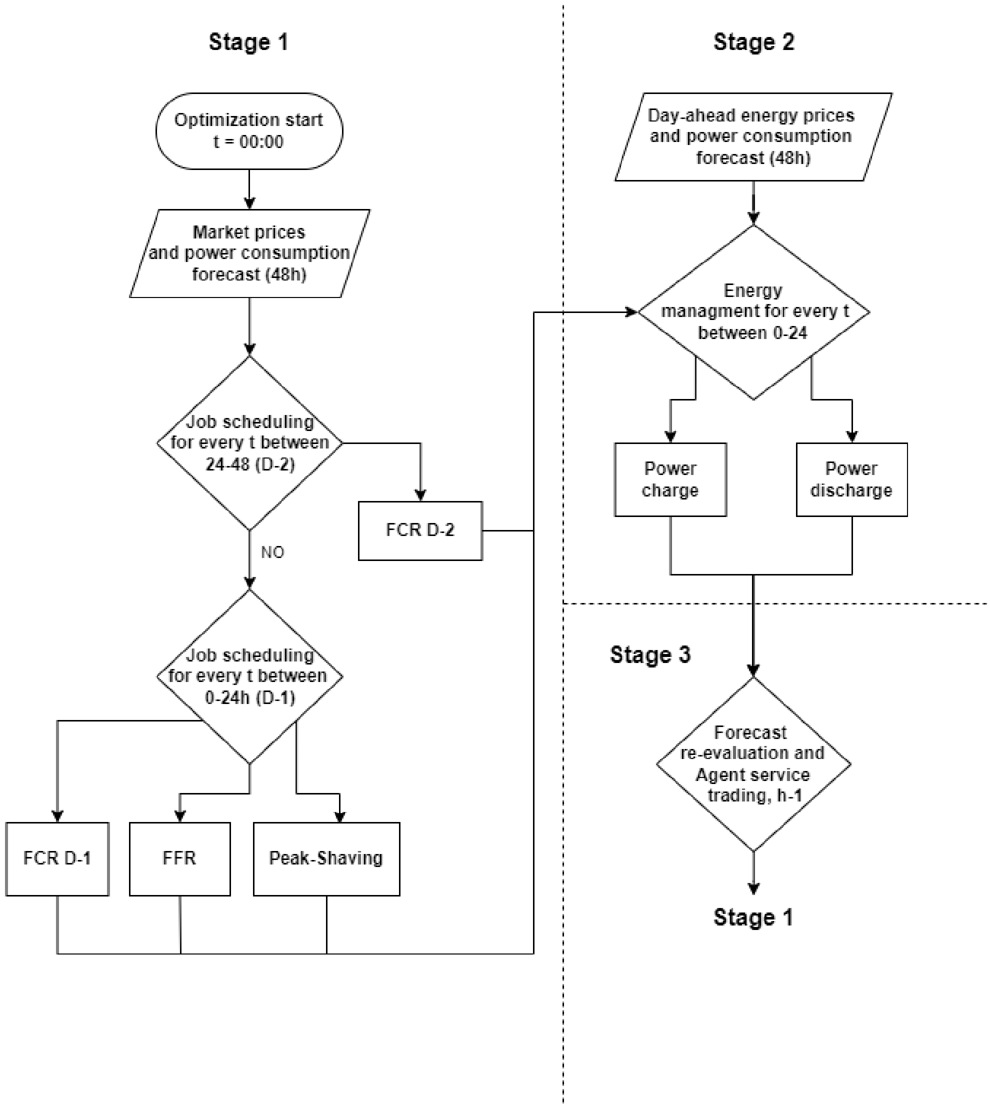

Figure 4.7: Optimization stages.

4.8.1 Stage 1 optimization: Job scheduling

The first stage of the optimization is a job scheduling problem. The job scheduling optimization is designed to allocate the time of the individual batteries to perform certain services for every hour, 48 hours ahead. The services allocated in this stage are FCR D-1, FCR D-2, FFR and peak-shaving participation. The objective function aims to maximizing profits during each hour, 48 hours ahead. For the objective function to maximize profits, each service has to have a known value for performing the service. Since market prices are assumed to be known for this project, the value of the reserve market participation can be derived from Equation 4.4.

$$V_t^{FCR-D1} = P^{max} \cdot C_t^{FCR-D1} \tag{4.4a}$$

$$V_t^{FCR-D2} = P^{max} \cdot C_t^{FCR-D2} \tag{4.4b}$$

$$V_t^{FFR} = P^{max} \cdot C_t^{FFR} \tag{4.4c}$$

where P^{max} is the power rating provided by the agents battery system, C_t^{FCR-D1}, C_t^{FCR-D2}, C_t^{FFR}, V_t^{FCR-D1}, V_t^{FCR-D2} and V_t^{FFR} is the price and value at hour t for participation in the specific reserve markets. Note that the value of reserve market participation is proportional to the power rating of the battery system. Different agents will therefore experience different values to reserve market participation services depending on battery size. Although, the reserve market prices are the same for all the agents, which means that the agents that will provide reserve market capacity will all participate in the same reserve market at a certain hour. The importance of this fact will become apparent in Section 4.8.3.

Calculating the value of peak-shaving participation is less trivial because the value is proportional to the future power consumption, which is stochastic. The value of the peak-shaving service can therefore not be deterministic, but needs to be analyzed using a probabilistic approach. The method of determining the value of the peak-shaving service in this project is to look at the direct costs of not providing the service. As explained in Section 3.3.1, if the power consumption of an agent exceeds a capacity step at a single hour in the month, the utility tariff increases by an amount specified in Table 3.1. The model therefore has to determine three important metrics; the Gaussian distribution of the forecasting error, the monthly capacity step at which the battery system realistically can peak-shave and the cost of entering a higher capacity step. The capacity step, $\bar{\alpha}_m$, at which the battery system can peak-shave also has to be calculated using a probabilistic approach. Different strategies of determining the monthly capacity step is discussed in Section 6.2.1. The different strategies could have benefits depending on the characteristics of the consumption profile. To determine $\bar{\alpha}_m$, the agent needs to know the probability of the consumption breaching a capacity step during the month, $P(\bar{\beta}_m)$, and if it is possible for the battery system to peak-shave to a lower capacity step. If the model assumes that the consumption every hour is independent of the consumption in other hours, the probability of a capacity step being breached during a month is a product of the probability of the capacity step being breached each hour. In statistical terms, the model could assume that the events, hourly capacity step breach probability, are independent as shown in Equation 4.5 and the monthly capacity step breach probability can be calculated.

$$P(\bar{\beta}_1 \cap \bar{\beta}_2 \cap ... \cap \bar{\beta}_{n-1} \cap \bar{\beta}_n) = P(\bar{\beta}_m) = P(\bar{\beta}_1) \cdot P(\bar{\beta}_2) \cdot ... \cdot P(\bar{\beta}_{n-1}) \cdot P(\bar{\beta}_n) \tag{4.5}$$

where n is the total number of hours in the month. Using Equation 4.5 to calculate the probability of breaching every capacity step will yield an array of $\bar{\beta}_m$. Table 4.2 shows a table of the probability of the consumption being under each capacity step for an entire month, $(1 - \bar{\beta}_m)$.

Capacity step[kW]	Com. building 1 [%]	Com. building 2 [%]
5	0	0
10	0	0
15	0	0
20	0	0
25	0	$2.46 * 10^{-102}$
50	$2.12 * 10^{-9}$	$1.27 * 10^{-6}$
75	93.25	5.28
100	100	26.98
150	100	56.96
200	100	72.38

Table 4.2: Total probability [%] of consumption being under each capacity step for the entire month, commercial building 1 and 2.

The method of finding the probability of breaching a capacity step described in Equation 4.5 assumes that the power consumption every hour is an independent event and that error distribution for every hour is the same. Both of these assumptions are not completely accurate. The power consumption one hour is highly correlated with the consumption in previous hours due to increased or decreased activity for the day. The MAPE error distribution of the forecast is larger when the consumption is lower because the same absolute error would have a larger percentage impact. Therefore, the average Gaussian distribution of the error is not entirely accurate representation for every hour of the day. The values in Table 5.3 are therefore not the actual probability of being under certain capacity levels. The values do, although, give an accurate indication of how many consumption data points are close to the specific capacity step. By testing, the model found that a realistic monthly capacity step can be determined when the total probability of breaching the capacity step is under 10^{-50}%.

When the monthly capacity step that the agent wants to peak-shave at is determined, the Gaussian error distribution and cost of a higher capacity step can be used to derive the formula for the value of the peak-shaving service.

$$P(X \leq \bar{\alpha}_m) = \int_{-\infty}^{\bar{\alpha}_m} f(p_t)\, dp_t = \frac{1}{\sigma\sqrt{2\pi}} \int_{-\infty}^{\bar{\alpha}_t} e^{-\frac{1}{2}(\frac{p_t - \mu}{\sigma})^2}\, dp_t \tag{4.6a}$$

$$V_t^{shave} = C^{cap} * P(X \leq \bar{\alpha}_m) = C^{cap} \cdot (1 - P(\bar{\beta}_t)) \tag{4.6b}$$

where $\bar{\alpha}_m$ is the monthly capacity step, μ is the error distribution mean, σ is the standard deviation and C^{cap} is the cost of entering a higher capacity step.

4.8.2 Stage 2 optimization: SOC planning

The second stage of the agent optimization aims to plan the SOC 24 hours ahead, specifically to allocate sufficient capacity to peak-shaving services and to perform energy arbitrage. As the model assumes that the minimum of 20% SOC is sufficient power to always participate in the reserve markets, the only SOC restrictions on performing energy arbitrage is the need to have sufficient power reserves to perform peak-shaving. In an optimization problem it is therefore necessary to restrict the minimum SOC at hours where the consumption has a high probability of exceeding the monthly capacity step.

The first step is to determine the needed SOC to perform peak-shaving. Since the power consumption is stochastic, the Gaussian error distribution of the forecast is therefore utilized to find the upper confidence interval. In forecasting, the confidence interval is often referred to as the prediction interval. In this model the base case upper prediction interval, $\hat{P}^{up}$, is set at 99.5%, meaning that 99.5% of consumption is going to be under the prediction interval. If the prediction interval exceeds the monthly capacity step the model will allocate energy to reduce peak consumption. The upper prediction interval is the leading factor to deciding what the minimum SOC should be to secure sufficient energy for peak-shaving services. If the upper prediction interval is set to a very high level, the agent would restrict the minimum SOC to a high level for more hours of the day to ensure peak-shaving capabilities. Restricting the minimum SOC to a high level would also give the battery agent less freedom to perform energy arbitrage since the minimum SOC acts as a constraint on the energy trading capabilities. In the stage 2 optimization the model first finds the needed energy for peak-shaving for each hour, 24 hours ahead, starting at midnight.

$$E_t^d = \hat{P}_t^{up} - \bar{\alpha}_m \qquad \forall t \in T_{24} \tag{4.7}$$

where E_t^d is the needed energy for peak-shaving given a 99.5% upper prediction interval. E_t^d can be negative, which will be used in Equation 4.8 to lower the minimum SOC before there is a need for peak-shaving.

The minimum SOC planning needs to consider the battery power rating, the total energy capacity and the needed energy for previous and subsequent hours. The minimum SOC planning consists of iterating backwards from the last hour to the first and adding the power demand to the minimum SOC based on the needed energy in the subsequent hours. The hours prior to the period of peak-shaving could also have a minimum SOC that is higher than the base case of 20% since the agent needs to be able to charge the battery without breaching the monthly capacity step and be charging within the power rating of the battery system. The concept can be observed in Figure 4.8. The minimum SOC can be calculated as seen in Equation 4.8.

$$SOC_t^{min} += SOC_{t+1}^{min} + \frac{E_t^d}{p^{max}} \qquad \forall t \in \{24, ..., 1\} \tag{4.8}$$

subject to:

$$E_t^d <= p^{max}$$
$$0.2 <= SOC_t^{min} <= 0.8$$

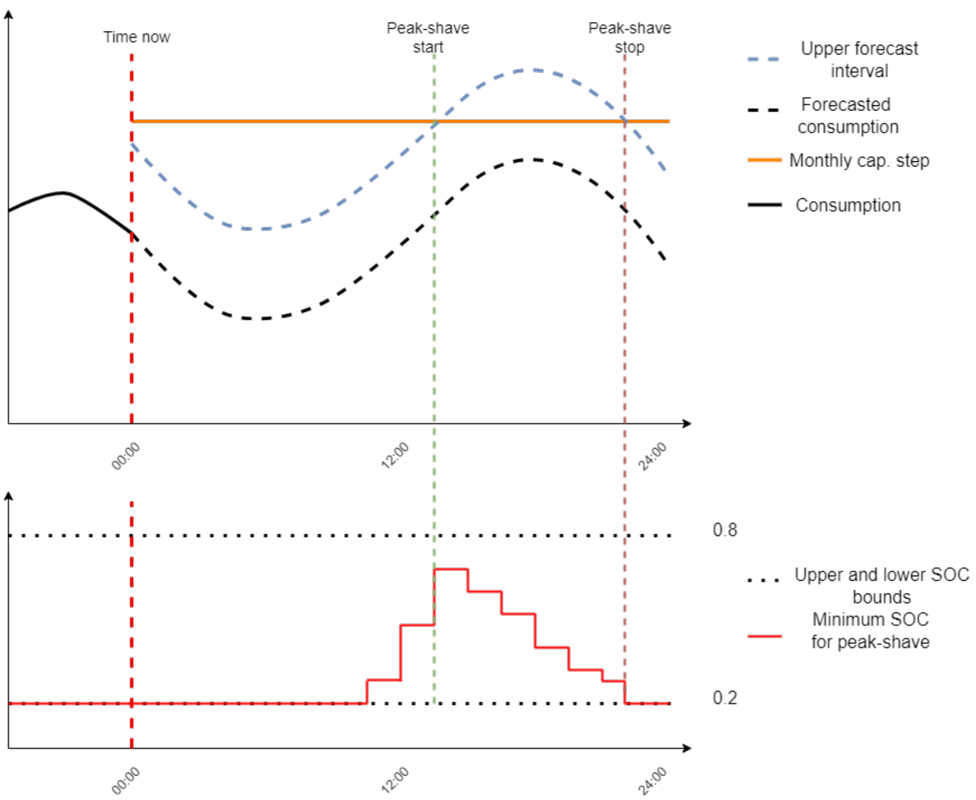

Figure 4.8: Minimum SOC allocation for peak-shaving and energy arbitrage service optimization using consumption forecast and prediction interval.

Figure 4.8 shows the principle of determining the minimum SOC to act as a constraint in an optimization problem for allocating energy for peak-shaving service. Take note that only the upper forecast interval is breaching the monthly capacity step. If the forecast is correct in the prediction the minimum SOC would be at 0.2 the entire time in Figure 4.8. Since forecasts are stochastic and the costs of breaching the monthly capacity step are so high, the model will allocate energy using the upper forecasting interval rather than using the true consumption forecast. The clear advantage of this strategy is that it uses the forecasting error to ensure peak-shaving capabilities despite deviations from the forecast. The disadvantage is that the minimum SOC constraint restricts the freedom of the agent to trade energy to a larger degree, and hence reduces energy arbitrage revenue. The upper prediction interval of 99.5% is therefore tunable and can be adjusted to maximize revenue for a specific agent.

When performing energy arbitrage, the optimization to maximize profits becomes more complex when there are varying SOC bounds. Figure 4.9 shows the relationship between the day ahead energy prices and a 24 hour, optimal SOC plan given SOC bounds.

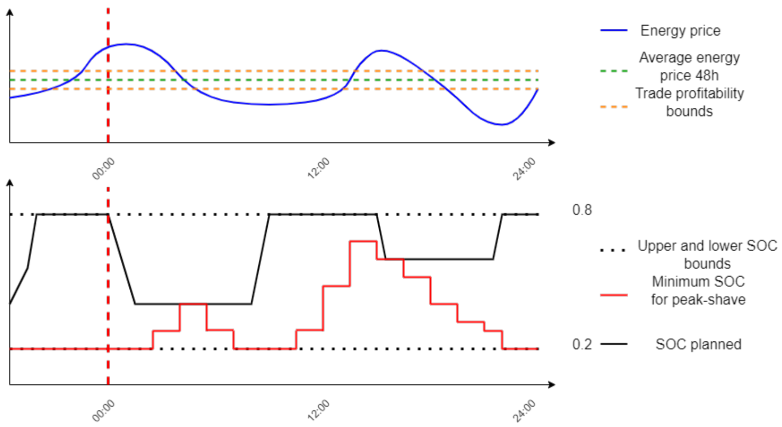

Figure 4.9: SOC planning for energy arbitrage service optimization with minimum SOC constraints.

To plan the optimal SOC 24 hours ahead, there are several variables that need to be determined. First, the model gives a buy- and sell value to the prices on the day ahead market. There is an assumed 5.13% base case loss on both the charge- and discharge operation. Hence, the prices on the day ahead markets need to vary by more than 5% from the price mean for energy arbitrage to be profitable. The value of buying and selling energy can be calculated.

$$V_t^{E,in} = p_t^{in} \cdot (\frac{C_{48}^{E,avg}}{C^{loss}} - C_t^E) \tag{4.9a}$$

$$V_t^{E,out} = p_t^{out} \cdot (C^{loss} \cdot C_t^E - C_{48}^{E,avg}) \tag{4.9b}$$

subject to:

$$\begin{aligned} &p_t^{in} <= p^{max} \\ &p_t^{out} <= p^{max} \\ &SOC_t^{min} <= p_t^{out} <= 0.8 \qquad\qquad p_t^{in} <= p^{max} \end{aligned} \tag{4.9c}$$

where $C_{48}^{E,avg}$ is the average price, 48 hours ahead, C_t^E is the price on the day ahead market, C^{loss} is the loss constant of 1.05, p_t^{in} and p_t^{out} is the available power to charge and discharge given SOC bounds. Equation 4.9a uses the average energy price the next 48 hours as a reference to know the value of energy in the future so the agent knows whether to sell, charge or be idle. The model uses the average energy price the next 48 hours because the model assumes the user consumption has daily consumption variations, so the agent will have possibilities to charge and discharge at lease once during the 48 hours. The SOC planning is only 24 hours ahead (D-1) while the energy price average is 48 hours ahead (D-2). This allows the agent to plan the energy arbitrage more precisely. If the energy prices in D-1 are lower than the energy prices in D-2, the agent will buy more energy in D-1 and will sell more energy in D-2. The SOC planning will likely result in the SOC being high at the end of D-1 in anticipation of higher prices. The opposite happens if the prices in D-2 are lower than the prices in D-1.

An LP optimization strategy is implemented to optimize buying and selling on the day ahead energy market. The optimization problem can be described as follows:

$$Maximize: \quad V_1^{E,in} \cdot x_1^{buy} + V_1^{E,out} \cdot x_1^{sell} + ... + V_{24}^{E,in} \cdot x_{24}^{buy} + V_{24}^{E,out} \cdot x_{24}^{sell}$$

$$\begin{aligned}
Subject\ to: \quad & SOC^{start} + x_1^{buy} - x_1^{sell} && \leq SOC^{max} \\
& SOC^{start} + x_1^{buy} - x_1^{sell} + x_2^{buy} - x_2^{sell} && \leq SOC^{max} \\
& ... && \\
& SOC^{start} + x_1^{buy} - x_1^{sell} + ... + x_{24}^{buy} - x_{24}^{sell} && \leq SOC^{max} \\
& SOC^{start} + x_1^{sell} - x_1^{buy} && \leq SOC_1^{min} \\
& SOC^{start} + x_1^{sell} - x_1^{buy} + x_1^{sell} - x_1^{buy} && \leq SOC_2^{min} \\
& ... && \\
& SOC^{start} + x_1^{sell} - x_1^{buy} + ... + x_{24}^{sell} - x_{24}^{buy} && \leq SOC_{24}^{min} \\
& x_1^{buy} \geq 0,\ x_1^{sell} \geq 0,\ ...,\ x_{24}^{buy} \geq 0,\ x_{24}^{sell} \geq 0 &&
\end{aligned}$$

where x_t^{buy} and x_t^{sell} are the buy and sell volumes. Since the value of buying energy, $V_t^{E,in}$, is directly contrary to the value of selling energy, $V_t^{E,out}$, and the LP will therefore not buy and sell at the same hour. Solving the LP problem results in a 24 hour ahead plan of the SOC to optimally buy and sell energy.

4.8.3 Stage 3 optimization: Agent job rescheduling and trading

The stage 3 optimization circumvents the restrictive rules on the reserve markets by trading peak-shaving and reserve market services between the agents on a self-developed local market. The trading on the local market is performed every hour. The agents therefore have an opportunity to adjust their consumption forecast and re-evaluate the value of the services. The main function of the stage 3 optimization is to increase agent profits by increasing flexibility and cooperation between the distributed agents. For the agents to trade services, there needs to be a change in circumstances that changes the value of the service being provided by the agents. For every hour ahead, the optimization needs to evaluate a new value of the peak-shaving service. The new value of the peak-shaving service is determined by evaluating the deviation between the actual consumption and the forecasted consumption for previous hours. This is used to update the forecast to increase accuracy. The model uses autoregression on the residual errors to correct the predictions.

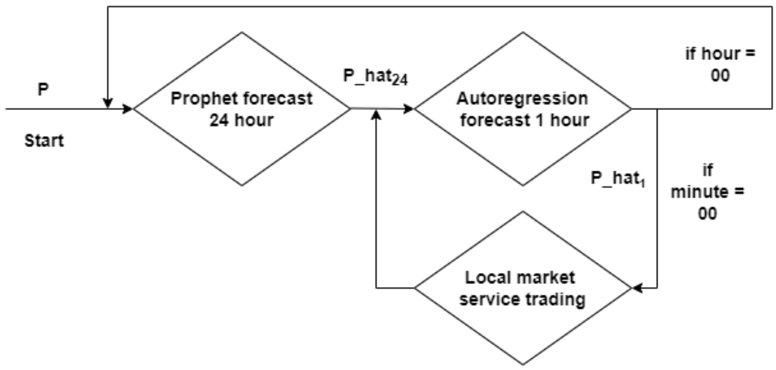

Figure 4.10: 1 hour forecast improvement using Autoregression for local market service trading.

Figure 4.10 describes the workflow and the process of updating the consumption forecast every hour and perform market service trading between the agents. The "if hour = 00" indicates that the time has reached 12AM and therefore enters a new day with the need for a new 24 hour Prophet forecast. The "if minute = 00" indicates the start of a new hour and therefore the need for a 1 hour autoregression forecast. The autoregression is calculated using the process described in Equation 4.10.

$$\varepsilon_t = \frac{P_t - \hat{P}_t}{P_t} \tag{4.10a}$$

$$\varepsilon_{t+1} = b_0 \cdot \varepsilon_t + b_1 \cdot \varepsilon_{t-1} + ... + b_n \cdot \varepsilon_{t-n} \tag{4.10b}$$

$$\hat{P}^{auto}_{t+1} = \varepsilon_{t+1} \cdot \hat{P}^{Proph}_{t+1} \tag{4.10c}$$

where ε is the residual error and $\hat{P}$ is the forecasted consumption. In principle, autoregression analyses the error between historical predicted and actual consumption values to provide an improved forecast based on weighted error coefficients. Using the 'statsmodels' Python library for autoregression, the coefficients,

b_n, are calculated. Since the consumption the last hour is the most accurate indicator of future consumption, b_0 is the highest weighted coefficient. The hourly ahead forecast increases the forecasting accuracy significantly since forecasting one hour ahead is more predictable than forecasting 24 hours ahead.

Every agent uses their updated, 1 hour forecast, $\hat{P}_{t+1}^{auto}$, to calculate the new value of the possible services they can provide. The value of the peak-shaving service has not changed since the reserve market prices for the hour and the agent battery power rating is constant. As mentioned in 4.8.1, every agent that is participating in the reserve market at a certain hour is participating in the same market. This is useful in the market clearing process where there will be only supply and demand. In this model, energy arbitrage services happens independently and is in this thesis not tradable between agents. The agents battery system is assumed to always be able to provide the energy that is bid on the day-ahead market as planned in the stage 2 optimization. The agents that are trading in the local market will therefore only be trading the peak-shaving and reserve market service obligations. The trading of the services happens using a traditional supply and demand curve, where the intersection between the curves decides the clearing price and the traded volume. Figure 4.11 shows an example of a market clearing event.

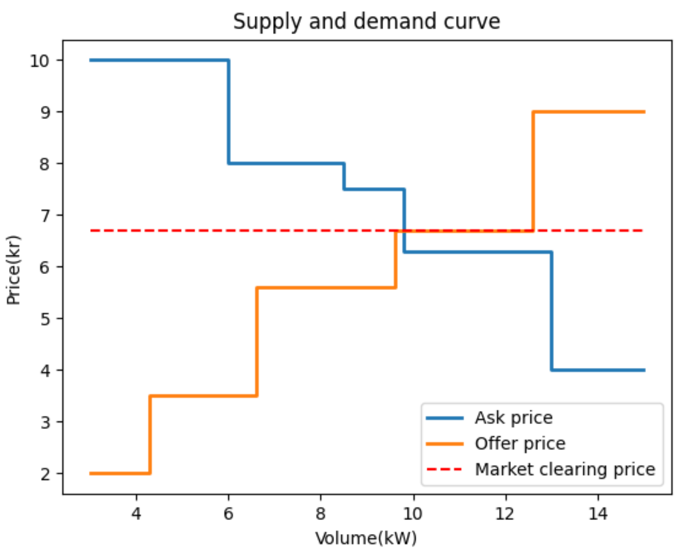

Figure 4.11: Supply and demand market clearing process.

The ask price and offer price in Figure 4.11 are the demand and supply bids, respectively. Figure 4.11 shows a common strategy in energy markets for determining the market clearing price based on a free market where there are market participants supplying a service and there are market participants demanding a service. The model will be using the "price as clear" methodology, which allows agents to enter their marginal cost bids and reduces the need for tactical bidding from the agents. Using the principles presented in Figure 4.11, the model implements a trading strategy between the agents using a supply and demand structure. The service being supplied and demanded is as follows:

- Demand - Due to an increase in power consumption compared to the forecast, an agent that is providing reserve market services the next hour is asking (demanding) other agents to relieve them of their obligations to the TSO by providing power reserves. The agent is willing to pay a certain amount for another agent to relieve them of their obligations, so they themselves can provide peak-shaving services.
- Supply - An agent that is providing peak-shaving services the next hour can supply other agents with the service of relieving their obligations to the TSO by providing power reserves.

The agents that supply create a bid regardless if the updated forecast is higher or lower than the original forecast. For a large enough compensation, the agents are willing to perform trades. The bids on the local market are calculated by updating the peak-shaving values, $V_t^{shave,new}$, of every agent using Equation 4.6b and using the value of reserve market participation.

$$V_t^{res} = max(V_t^{FFR}, V_t^{FCR-D1}, V_t^{FCR-D1}) \tag{4.11a}$$

$$S_t^a = \begin{cases} 0 & \text{if } SOC_t = SOC_t^{min} \\ \frac{2 \cdot V_t^{shave,new} - V_t^{res}}{P_{max}} & \text{otherwise} \end{cases} \tag{4.11b}$$

$$D_t^a = \frac{V_t^{shave,new}}{P_{max}} \tag{4.11c}$$

where S_t^a and D_t^a is the supply and demand bids, respectively. The supply bid is set to 0 when the SOC is at the minimum bound, because the battery system is incapable of peak-shaving when the SOC is at minimum charge. The market clearing price is set at the intersection between the supply and demand curve. This maximizes social welfare which is desired in free markets. If the supply and demand curves do not intersect, there will be no market clearing price and therefore no trades will be executed.

4.9 Simulation interface

To verify the results, a Graphical User Interface (GUI) has been implemented in the model to visualize the simulations. The GUI is used as a visual tool to analyse the model output data and verify the feasibility of the results. The interface shows four subplots that provide useful information on the results in the optimization process. A GIF showing the first 72 hours of the base case simulation animation can be found using this hyperlink: Click here

Or follow this link:
`https://studntnu-my.sharepoint.com/:f:/g/personal/abrahaps_ntnu_no/EiOJs1ZjhrxMrtKvj60oTaABSMfPzg2tFYEZTdRe30fn4Q?e=nvq7J1`

Figure 4.12 shows a screenshot of the simulation. To get a larger figure of the GUI follow the same link as above.

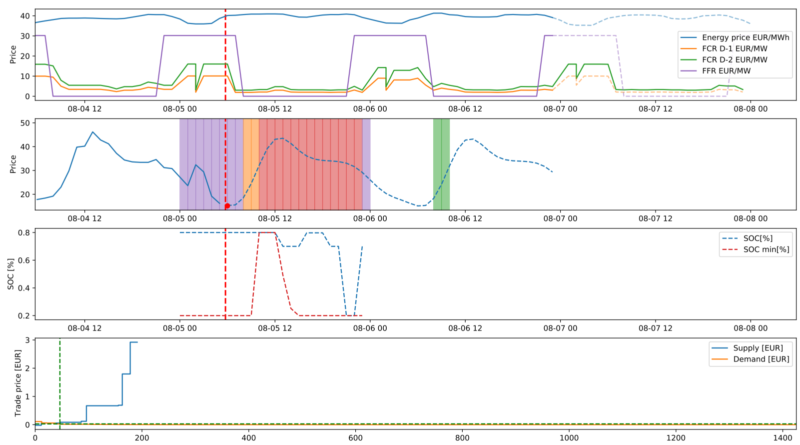

Figure 4.12: Simulation GUI for commercial building 1.

The vertical, dotted red line indicates the time now.

4.9.1 Subplot 1: Market prices

The first subplot shows the market prices of the day ahead market, FCR D-1, FCR D-2 and FFR markets. The day ahead prices are given in EUR/MWh and the other markets are given in EUR/MW. As mentioned, this thesis assumes that the market prices are known. The dotted lines show the prices that are not yet cleared. This can be observed by looking at the FCR D-2 market that gets cleared a day before the other markets.

4.9.2 Subplot 2: Job schedule and power consumption forecast

The second subplot shows the job scheduling, the recorded consumption and the forecasted consumption of the specific battery owner. The recorded consumption is in a solid, blue line. The time slots are shaded in different colors representing the service that is being provided.

- Red - Peak-shaving service allocation.
- Purple - FFR service allocation.
- Orange - FCR D-1 service allocation.
- Green - FCR D-2 service allocation.

Notice how the agent wants to perform peak-shaving services when the consumption forecast is high and wants to perform reserve market participation at hours where the consumption is expected to be low. The job scheduling in subplot 2 in Figure 4.12 shows that two days ahead only two hours are allocated to the FCR D-2 market. This is because the agent expects other services to have more value that day, so only the D-2 service needs to be allocated at that time if it is expected to be the most profitable. There is a red dot that is after the time now line. This dot indicates the updated, one hour forecast described in Section 4.8.3.

4.9.3 Subplot 3: SOC planning

The third subplot shows the planned SOC with the minimum SOC of the specific battery system. This subplot shows when the battery system has allocated energy to peak-shaving by increasing the minimum SOC bound. In Figure 4.12, through the optimization process, the agent has kept the SOC high to adhere to the minimum SOC bound. After the minimum SOC bound is reduced again, the agent decides to sell energy when the price is high and buy energy before the end of the day because the energy price is below the average energy price.

4.9.4 Subplot 4: Local market trading

The fourth subplot shows the trade of services between agents. As described in Section 4.8.3, the services are represented in a supply and demand curve. The clearing price and clearing volume is shown by a dotted green line and is at the intersection between the supply and demand curves. All the agents on the left side of the vertical green line has traded services with each other.

4.10 Simulation scenarios

The simulations are run for an entire year to determine the revenue stream from the different services. The market data from 2019 is used for the simulations, since there is more consumption data from 2019. The simulations will therefore become more complete and reliable. There are also only one year simulations because of the computational time the simulations require.

4.10.1 Base case

The base case scenario uses only the consumption data from commercial buildings 1 and 2, and the aggregated areas. Otherwise, the scenario runs a simulation using the model described in the thesis.

4.10.2 Scenario 1: Additional large consumers

In scenario 1, there are an additional four consumers that are added to the consumer data set. These users have a much larger consumption as can be observed in Table 4.1. Especially the factory has an average power consumption of 3667 kW, which is around 100 times larger than the consumption of the average base case users. This scenario will analyse how the model is utilized by larger consumers. The results will indicate how the model wishes to utilize the battery system when it is connected to a larger consumer.

4.10.3 Scenario 2: C-rating change

In scenario 2, the C-rating is changed from 0.5 to 1. This essentially means that if a battery system in the base case had a rating of 10kWh/5kW, it now has a rating of 10kWh/10kWh. Realistically, increasing the power rating would require improved power electronics in the battery system. This would realistically cost more, but a C-rating of 1 is common for battery systems. The aim with this scenario is to analyse the how much the revenue increases when the power rating increases.

4.10.4 Scenario 3: FFR removed

In scenario 3, the FFR market is removed. As explained in Section 3.4.2, the FFR market is based on a market test. The market is not active at the time of writing this thesis. Therefore, realistically, a battery system cannot bid on the market at this time. Removing the FFR market gives an indication on how the battery system would perform in a the current market conditions. Note that the monthly utility power tariff is not implemented as the time of writing this thesis, but the DSOs in Norway are looking to implement the tariff within year 2022. The power tariff is therefore still active in this scenario.

4.10.5 Scenario 4: 2021 energy prices

In scenario 4, the energy prices on the day ahead market for 2021 will be used in the simulation. The reason this analysis is interesting is that the energy prices towards the end of 2021 rose significantly due to the price increase of natural gas and crude oil. The winter in Norway was also very dry, causing the water reservoirs to deplete, further increasing the energy prices. The energy arbitrage service revenue is directly effected by the fluctuations in price. When there are large differences between the lowest and highest energy prices during the day, the battery system can exploit this to earn a profit. Many analysts expect energy prices to remain high in the future. This scenario will therefore analyse the model performance if this is the case.

Chapter 5

Results

In this chapter the results from the model is presented. Section 5.1 presents results of the Prophet forecasting accuracy in the model. Section 5.3 presents the results for the different scenarios. To give a structured representation of the results, the results for the scenarios are presented in the same format.

5.1 Prophet consumption forecasting

The Mean Average Percentage Error (MAPE), Mean Average Error and Mean Square Erro (MSE) is calculated for 10 different consumers to give insight into the performance of the Prophet forecasting algorithm. The results of the error calculations for the 48 hour forecasts are presented in Table 5.1.

Consumer	MAPE	MAE	MSE
Commercial building 1	0.0868	3.28	20.5
Commercial building 2	0.258	5.79	56.6
Aggregated area 3	0.109	3.63	21.1
Aggregated area 7	0.0878	7.17	82.5
Aggregated area 23	0.0805	3.67	22.3
Aggregated area 41	0.0891	4.45	32.0
Factory	0.0466	178	51400
Condominium	0.0848	9.91	164
Store 1	0.166	37.9	2480
Store 2	0.317	57.5	5510

Table 5.1: MAPE, MAE and MSE of 10 consumers using the Prophet algorithm.

There is a relatively large discrepancy in forecasting performance between the consumers. Forecasting for commercial building 1 has a substantially better MAPE, MAE and MSE of 0.0868 compared to commercial building 2 with 0.258. The aggregated areas have a fairly consistent MAPE between 0.08 to 0.11. The factory has a very low MAPE, but has a very high MAE and MSE, which is expected when the average consumption of the factory is high. Store 1 and store 2 have a high MAPE, MAE and MSE. Given the error calculations presented in Table 5.1, the error deviation can be plotted for consumers with accurate and inaccurate consumption forecasts. Figure 5.1 shows the forecast deviation for commercial building 1 and Figure 5.2 shows the forecast deviation for commercial building 2.

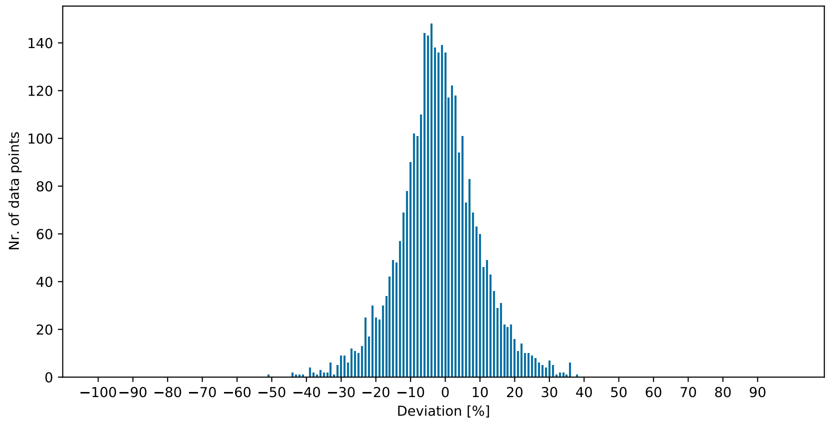

Figure 5.1: Forecast deviation from actual values, Commercial building 1.

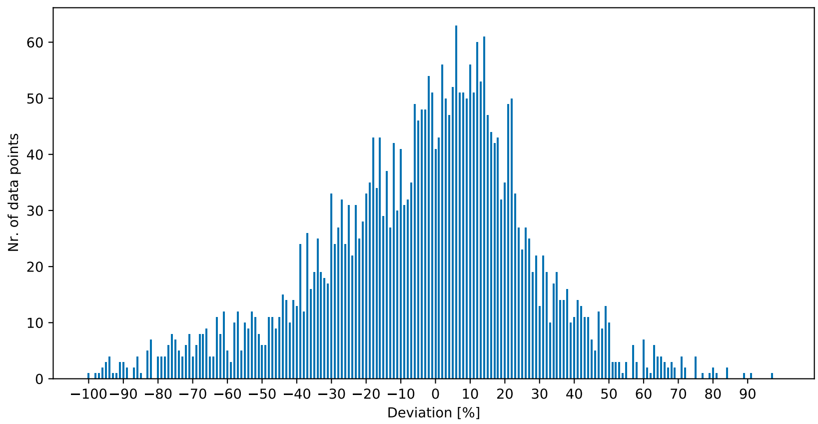

Figure 5.2: Forecast deviation from actual values, Commercial building 2.

As can be seen in Figure 5.1 and 5.2, the Prophet forecasting algorithm has much larger success with commercial building 1 than commercial building 2. The reason behind this is discussed in Section 6.1.1. The peaks of the error deviation is not perfectly centered at 0%, which could indicate that the forecast is either overdamped or underdamped, and that the forecast has difficulties forecasting local peaks.

5.2 Optimization

5.2.1 Peak-shaving optimization

When the monthly capacity step is to be determined, the probability of the consumption being under a capacity step is calculated. This calculation is performed for every hour the following month, but a 10 hour example for commercial building 2 is shown in Table 5.2.

Time[h]	Power[kW]	5kW	10kW	15kW	20kW	25kW	50kW	75kW
14:00:00	18.2	0.0	1.5	22.3	63.6	88.8	99.0	99.5
15:00:00	17.1	0.0	2.7	29.7	73.6	92.2	99.1	99.6
16:00:00	14.1	0.0	9.4	58.7	91.1	96.4	99.3	99.7
17:00:00	10.6	0.0	39.5	90.4	96.9	98.5	99.6	99.9
18:00:00	8.7	2.2	70.1	95.7	98.2	99.1	99.7	99.9
19:00:00	9.2	1.2	61.9	94.5	98.0	99.0	99.7	99.9
20:00:00	11.2	0.0	32.4	87.2	96.4	98.1	99.6	99.8
21:00:00	13.2	0.0	14.0	68.7	93.1	96.9	99.4	99.7
22:00:00	14.6	0.0	7.4	54.0	88.8	95.7	99.2	99.7
23:00:00	16.0	0.0	4.3	38.4	81.4	93.7	99.2	99.6

Table 5.2: Probability [%] of consumption being under each capacity step for 10 time steps, commercial building 2.

Commercial building 2 has an inaccurate forecast, which reflects in the calculations for the capacity step calculations. Table 5.2 shows that even though the consumption forecast is between 8.7 to 18.2, the forecast for commercial building is never 100% certain that the consumption will be under 75kW.

As described in Section 4.8.1, the monthly capacity step for an agent is decided using the compounded probabilities of breaching the capacity step for the month. This is done by multiplying all hourly probabilities for the month. In other words; multiplying all the hourly column values in Table 5.2 yields the probability of being under the capacity step for the month. Table 5.3 shows the monthly probabilities of being below all the monthly capacity steps for commercial building 1 and 2. The monthly capacity step is decided by the first capacity step that has higher than 10^{-50}% probability. This probability is confirmed by tests and simulations.

An example of the determined reserve market bid as a result of Equation 4.6b is presented in Table 5.4 and 5.5. The value of the peak-shaving service increases linearly with the probability of breaching the monthly capacity step.

Capacity step[kW]	Com. building 1 [%]	Com. building 2 [%]
5	0.00	0.00
10	0.00	0.00
15	0.00	0.00
20	0.00	0.00
25	0.00	0.00
50	$2.12 * 10^{-9}$	$1.27 * 10^{-6}$
75	93.25	5.28
100	100	26.98
150	100	56.96
200	100	72.38

Table 5.3: Total probability [%] of consumption being under each capacity step for an entire month, commercial building 1 and 2.

Time	Cons. forecast[kW]	Cap. level prob. [%]	Peak-shaving value [EUR]
07:00	19.96	100.00	0.000
08:00	23.04	100.00	0.000
09:00	28.88	100.00	0.000
10:00	36.12	98.84	1.217
11:00	42.59	92.10	8.285
12:00	46.50	78.46	22.59
13:00	47.29	73.54	27.75
14:00	45.70	83.51	17.29
15:00	43.09	91.13	9.298
16:00	40.58	95.52	4.693

Table 5.4: Reserve market bid compared to consumption forecast and under 50kW capacity level probability for 10 hours, commercial building 1.

Time	Cons. forecast[kW]	Cap. level prob. [%]	Peak-shaving value[EUR]
07:00	20.06	98.69	1.366
08:00	23.83	97.73	2.375
09:00	25.81	97.11	3.029
10:00	25.61	97.28	2.850
11:00	24.41	97.56	2.553
12:00	23.71	97.90	2.197
13:00	23.81	97.73	2.375
14:00	23.49	97.90	2.197
15:00	21.21	98.49	1.573
16:00	16.75	99.12	0.9206

Table 5.5: Reserve market bid compared to consumption forecast and under 50kW capacity level probability for 10 hours, commercial building 2.

The importance of forecasting accuracy becomes apparent when observing table 5.4 and 5.5. From table 5.1 it is concluded that commercial building 1 has a higher consumption forecasting accuracy than commercial building 2. Commercial building 1 has several 0 EUR bids. This is due to the forecasted consumption being less than 30kW, which is 40% less than the relevant capacity step of 50kW. The forecast has never historically deviated more than 40% from the actual consumption values, and the model is therefore confident the consumption will not deviate more in the future. The risks associated with reserve market participation rather than peak-shaving services are concluded to be negligible and the marginal cost will therefore be 0 EUR, resulting in a 0 EUR peak-shaving value. The closing price at the TSO will in many cases be higher than the bid provided by the central controller, providing a margin of safety for the agents.

5.2.2 Cost of flexibility

Lede AS, which is a DSO, has specifically requested an analysis of what the cost of flexibility is at certain times. The reason is that in a free market environment, it would be useful to know how much flexibility would cost for the DSO if they were to establish their own market or if they were to rent services from a flexibility provider. In the model developed, the agents of the battery systems assigned a value to the service provided for each hour. Plotting the service values from cheapest to most expensive for 10 days provides Figure 5.3.

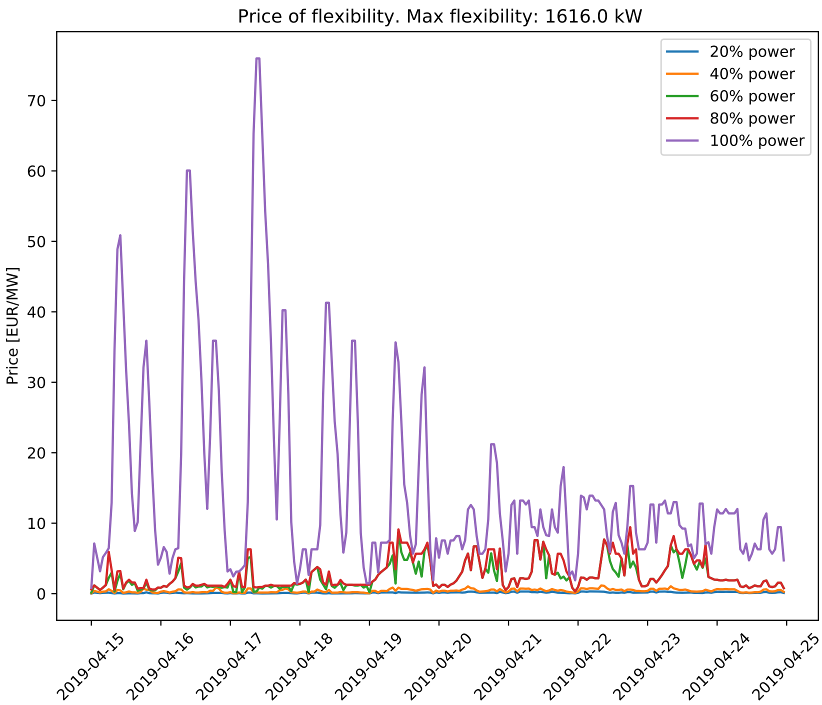

Figure 5.3: Flexibility cost from cheapest to most expensive.

Figure 5.3 shows that with a total of 1616 kW available power, there is a large disparity between the most expensive agents and the cheapest. The value of the services that the battery system provides are most expensive during the day due to the need for peak-shaving services. An interesting observation is that around 40% of the power capacity is always available at a comparably cheap price, likely because it was the reserve market prices that had the highest value for the agent. Therefore, outbidding the reserve markets could secure a relatively high amount of capacity if a DSO were to compete for the battery services.

5.3 Scenario presentation description

The following pages will show the results from the simulations performed on the base case model and the scenarios explained in Section 4.10. The results from the simulations are presented the exact same way for all the scenarios. This is to easily observe how the model reacts to the changing parameters. The results pages are split into two figures, two tables and six individual information boxes. It is advised to take a look at the base case results page before reading the description below.

The top left figure shows the amount of time the average battery system spent performing each service. The different colors represent the different services.

- Red - Peak-shaving
- Purple - FFR
- Green - FCR D-2
- Orange - FCR D-1

Since the figure only shows the average service allocation of the battery system, it can give a misleading impression of what all the agents do. The outer rings in the figure show the maximum percentage job allocation for the agents. In other words, if the closest, red outer ring is shaded 90% red, it means that at least one agent spent 90% of the time providing the peak-shaving service. The figure gives an indication of how much variation there is in service allocation amongst agents. The energy arbitrage service is not shown in the figure because the energy arbitrage service is being provided at the same time as other services.

The top right figure shows which services the revenue comes from. The energy arbitrage revenue is shown in blue. This figure shows which services are creating the largest value for the average battery owner. This figure can closely resemble the top left figure, but this is not always the case.

The two tables presented give useful output information from the model. The table to the left presents the same information shown in the figures. It is easier to observe small changes in the results when comparing the scenarios. The table to the right show the total energy rating when combining the energy rating of all the battery systems in the model. The total power rating for all the battery systems is also presented. The C-ratio in the base case is 0.5, meaning that the total power rating is half the total energy rating. The monthly revenue that is presented in the right table presents the total revenue the model earned using the battery systems. The right table also presents the revenue per kWh per month and the revenue per kW per month. This is an important metric when analysing investment opportunities. The different scenarios will indicate when the model becomes more profitable.

The six boxes on the result pages also presents useful information on the performance of the model. The "peak-shave success" box shows the percentage of agents that managed to reduce the monthly utility power tariff within the month. With the energy and power rating of the battery system being only 25%/12.5% of the maximum power consumption, it is not always possible to reduce the monthly utility power tariff, so a 100% peak-shaving success rate is unrealistic. The "Tot. energy traded" box shows the total amount of energy traded during an average month. This is both bought and sold energy that is in this statistic, so it is the total energy that has been cycled through the battery systems. The "Avg. price of flex" is what the average value of the service being provided is per hour. This also includes the value of the peak-shaving service, which does not have a direct monetary value at the point of service. The "Traded hours" shows the percentage of time an average battery system traded an hourly service to another service. In other words; it is the percentage of time that a service was booked for an hour, but the average battery system resulted in trading for another service on the local market in the central controller. The "Rev. inc. from trading" box shows how much the total revenue increased due to trading services on the local market. The "Trading val." box shows the total value traded on the local market, where the value is decided by the agents. Note that the agents are allocating a value to the service they are trading on the local market. This value is not a monetary gain in the form of increased revenue, but this value gives some insight into the intensity and volatility of the trading on this market.

5.4 Base case

The complete description of the results presented are found in Section 5.3.

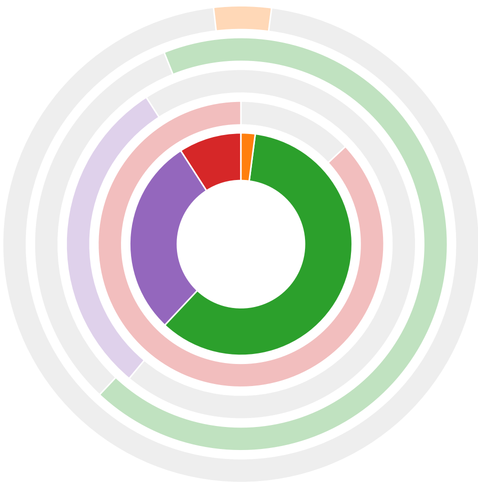

(a) Service allocation with max. agent service proportion.

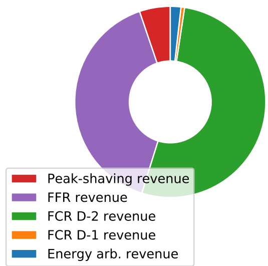

(b) Service revenue.

Service	**Jobs [%]**	**Rev. [%]**
Peak-shaving	9.0	5.2
FFR	28.9	40.0
FCR D-2	59.9	52.4
FCR D-1	2.1	0.6
Energy arb.		1.8

Metric	**Values**
Total energy rating	1514kWh
Total power rating	757kW
Monthly revenue	13263€
Rev./energy	8.76€/kWh
Rev./power	17.5€/kW

Peak-shave success	Tot. energy traded	Avg. price of flex
10.0%	62.0MWh	0.65€/h

Traded hours	Rev. inc. from trading	Trading val.
19.8%	0.26%	2256€

5.5 Scenario 1: Additional large consumers

The complete description of the results presented are found in Section 5.3.

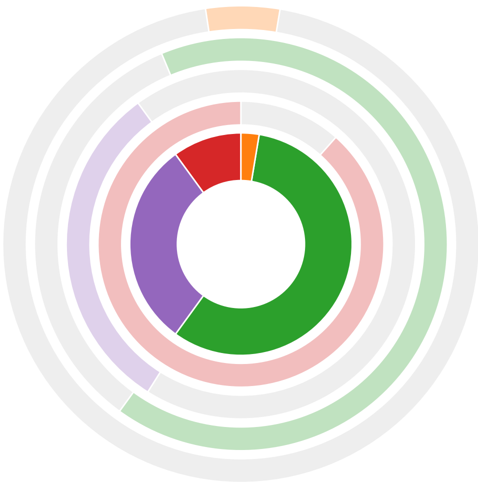

(a) Service allocation with max. agent service proportion.

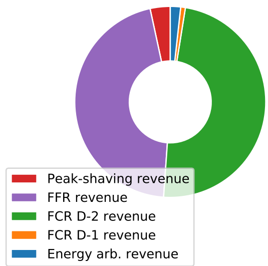

(b) Service revenue.

Service	Jobs [%]	Rev. [%]
Peak-shaving	10.0	3.4
FFR	30.0	45.5
FCR D-2	57.4	48.6
FCR D-1	2.6	0.8
Energy arb.		1.7

Metric	Values
Total energy rating	3232kWh
Total power rating	1616kW
Monthly revenue	25458€
Rev./energy	7.86€/kWh
Rev./power	15.8€/kW

Peak-shave success	Tot. energy traded	Avg. price of flex
9.27%	153.8MWh	1.04€/h

Traded hours	Rev. inc. from trading	Trading val.
24.0%	0.15%	2264€

5.6 Scenario 2: C-rating change

The complete description of the results presented are found in Section 5.3.

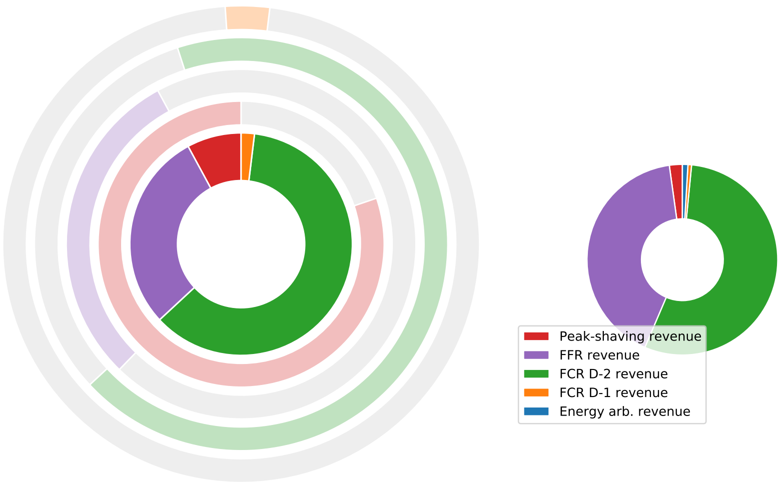

(a) Service allocation with max. agent service proportion.

(b) Service revenue.

Service	**Jobs [%]**	**Rev. [%]**
Peak-shaving	7.8	2.2
FFR	29.0	41.4
FCR D-2	61.1	54.9
FCR D-1	1.9	0.6
Energy arb.		0.9

Metric	**Values**
Total energy rating	1514kWh
Total power rating	1514kW
Monthly revenue	25801€
Rev./energy	17.0€/kWh
Rev./power	17.0€/kW

Peak-shave success	Tot. energy traded	Avg. price of flex
8.00%	61.6MWh	1.03€/h

Traded hours	Rev. inc. from trading	Trading val.
19.2%	0.10%	3011€

5.7 Scenario 3: FFR removed

The complete description of the results presented are found in Section 5.3.

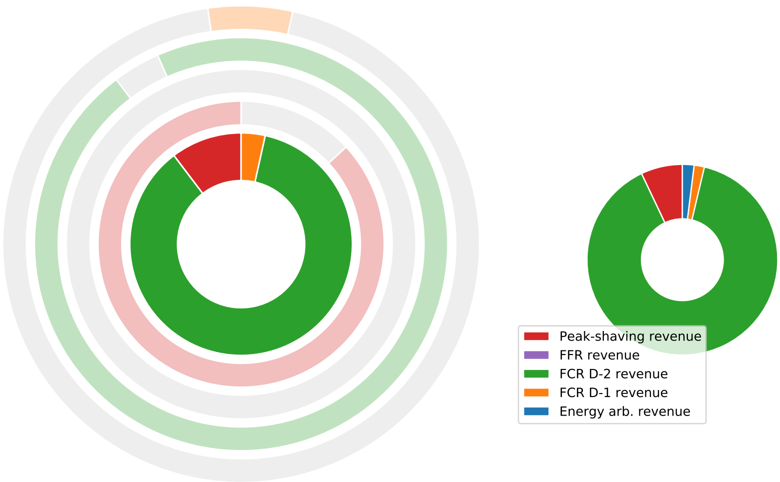

(a) Service allocation with max. agent service proportion.

(b) Service revenue.

Service	**Jobs [%]**	**Rev. [%]**
Peak-shaving	10.3	7.1
FFR	0	0
FCR D-2	8.6	8.9
FCR D-1	3.4	1.7
Energy arb.		1.9

Metric	**Values**
Total energy rating	1514kWh
Total power rating	757kW
Monthly revenue	9816€
Rev./energy	6.48€/kWh
Rev./power	13.0€/kW

Peak-shave success	Tot. energy traded	Avg. price of flex
10.00%	60.2MWh	0.84€/h

Traded hours	Rev. inc. from trading	Trading val.
20.9%	0.19%	2260€

5.8 Scenario 4: 2021 energy prices

The complete description of the results presented are found in Section 5.3.

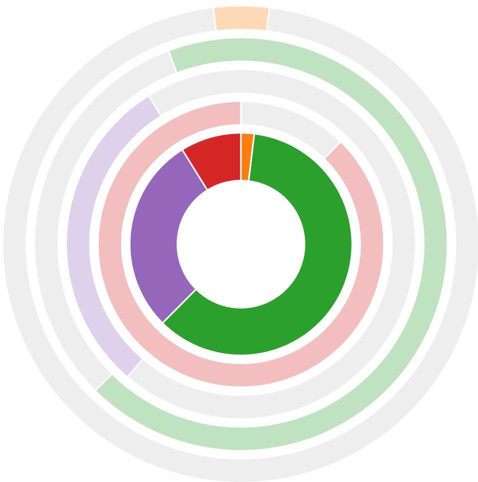

(a) Service allocation with max. agent service proportion.

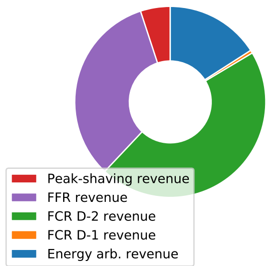

(b) Service revenue.

Service	**Jobs [%]**	**Rev. [%]**
Peak-shaving	8.9	5.0
FFR	28.7	32.9
FCR D-2	60.5	45.6
FCR D-1	1.9	0.5
Energy arb.		15.9

Metric	**Values**
Total energy rating	1514kWh
Total power rating	757kW
Monthly revenue	17143€
Rev./energy	11.3€/kWh
Rev./power	22.6€/kW

Peak-shave success

10.00%

Tot. energy traded

41.9MWh

Avg. price of flex

0.89€/h

Traded hours

19.1%

Rev. inc. from trading

0.18%

Trading val.

2141€

Chapter 6

Discussion

The discussion chapter in this thesis gives insight into the results presented in Chapter 5. The discussion chapter will give explanations as to why the scenarios changed the base case results. This chapter also discusses possible improvements to the model developed and discusses possible real-world application of the model. This chapter also discusses the market conditions in Norway and if battery systems are suitable for grid implementations.

6.1 Results discussion

6.1.1 Prophet forecasting

The Prophet forecasting algorithm is a useful plug-and-play tool for implementation in this model. The algorithm is designed to detect seasonal, monthly, weekly and daily trends. This is ideal for many power consumers in the grid. The algorithm is easy to tune if there are consumers with different characteristics. The algorithm is unfortunately not designed to quickly adapt to the power consumption characteristics of consumers with volatile changes in their power consumption pattern. The Prophet forecasting method is therefore not suited for consumers with irregular consumption patterns.

The differentiating forecasting performance is observed in Table 5.1. The forecasting accuracy is wildly different between commercial building 1 and commercial building 2. Commercial building 1 has extremely predictable consumption, while commercial building 2 has sporadic periods where the building is inactive without any clear reason or trend. The Prophet forecasting algorithm does allow for the creation of trend rules. For example; the building is closed every third Tuesday. This is a rule that the Prophet forecasting algorithm would not detect, but can be told to implement. For this thesis the customization of the forecasting towards individual consumers has not been a priority, but it could be done to increase accuracy of the forecasting.

Another issue with the Prophet forecasting algorithm is that the forecasting computational time increases exponentially with the input data size. The Prophet forecasting algorithm spent around 0.3 seconds with one month historical consumption data for one consumer, which is decent. When the Prophet forecasting method received 10 months with historical consumption, the computational time was around 10 seconds, which is substantially higher. The simulations was therefore extremely time consuming when there are 50 agents and they each have to update the forecasts every 24 hours. Other traditional regression based forecasting methods might have worse forecasting results, but could create forecasts much faster.

6.1.2 Base case

When running simulations on the base case, the battery priorities become apparent. The battery system spends the overwhelming amount of time performing reserve market services. Specifically, performing FFR- and FCR D-2 services is done 88.9% of the time. The peak-shaving service is performed around 9.0% of the time and FCR D-1 around 2.1% of the time. A good indication that the optimization model is working well is that the job scheduling closely reflects the revenue it produces. On average, the battery systems allocate 9% of the time to peak-shaving, which makes up 5.2% of the revenue. It is to be expected that there is a slight deviation between the percentage service scheduling and the total revenue the services makes since some of the services only produce a high value at certain hours. This is the reason that the FFR market creates the highest value compared to the time the battery system is active in the FFR market. The FFR market has a high price for only a few hours.

The outer lines on the job scheduling show that there are some agents that spend around 85% of the time peak-shaving. This is a direct result of the design behind the optimization. The agents that predominantly decided to peak-shave had a large forecasting error and could therefore never be sure if the consumption was going to exceed the monthly capacity step. This shows the importance of having an accurate consumption forecast, since if there is an inaccurate forecast the optimization problem will fear a breach of the monthly capacity step and will allocate more time to peak-shaving services. There are also agents that only perform reserve market services. This is because the power consumption of that agent is far away from breaching the monthly capacity step at all times.

The revenue per kW and kWh give an indication of the profitability of the model. Since there have been made many assumptions as to the performance of the battery system and to what the power market allows of operations, it is difficult to say anything definitive about the profitability of the model. With the current assumptions implemented the average battery system makes 8.67€/kWh per month and 17.5€/kW per month. To have something to compare to; At the time of writing article [45] the Tesla Megapack in Australia generated 17 million US dollars in the first 6 months of operations with a energy rating of 129MWh/100MW resulting in a monthly revenue of 22.0€/kWh and 28.3€/kW. The revenue in this model is lower than that of the Tesla Megapack, but as the flexibility markets in Australia have much larger prices, this is expected. Battery systems are rarely utilized, so comparing the results with implemented models is difficult.

The peak-shaving success rate is at 10%, which means that the battery system managed to reduce the monthly capacity step at 10% of the agents for the simulated months. While this sounds low there are several reasons why it is difficult to increase this rate much higher.

- The maximum power rating is not sufficiently high to reduce large spikes to a lower capacity level.
- The energy rating is not sufficiently high enough to peak-shave if the peak consumption level lasts for several hours. The energy in the battery system will be depleted.
- There is a large span between the capacity steps when the consumption becomes high. For example: The next capacity step after 50kW is 75kW. If the power consumption of the agent fluctuates between 50kW and 70kW, there is nothing the battery system can do to reduce the monthly capacity step.
- There is a sudden, unexpected increase in power consumption that breaches the monthly capacity step.
- The SOC at the time of peak-shaving is not high enough to successfully peak-shave.

Of all the bullets listed above, only the last one is the fault of the model implemented, since it is the models responsibility to plan for sufficient SOC at peak consumption hours. The other factors are the result of a battery system that is to small to sufficiently peak-shave. Note that in the simulations, peak-shaving has been neglected for many of the agents because reserve market participation is more profitable. Having a high peak-shaving success rate is therefore not a direct metric of the models performance, but is instead a reflection on the agents priorities.

There was an average of 62MWh traded for each month. To put that into perspective; the average battery system fully charged and discharged 20.7 times a month meaning that the batteries managed to successfully perform exploit the energy price swings and perform energy arbitrage. The prices on the day ahead market have been historically low and not volatile. The year of 2019, which this simulation ran on, is not exception. In scenario 4 the day ahead prices for the end of 2021 were used. These prices are higher and more volatile. In the base case, energy arbitrage collected 1.8% of the total revenue. This is not significant. As stated in Section 3.1.2, energy cycling through the battery is a factor in battery degradation. This has been excluded from optimization calculations, but in a real-world application, this would have to be a factor when the energy arbitrage revenue only makes up 1.8% of the total revenue.

The average price of flexibility was at 0.65€/h meaning that the maximum value of the services was on average 0.65€ for the hour. The larger battery systems have a much higher average price for flexibility since they receive more compensation if they provide reserve market services.

From simulations it is observed that larger battery systems were more active with reserve market participation than the smaller battery systems. The reason for this is that the larger battery systems get a larger payout from the TSO when providing more reserve capacity on the markets compared to the smaller battery systems. The larger consumers also have larger span between the capacity steps in the DSO utility power tariff, resulting in the battery system not being able to peak-shave and therefore choosing reserve market services instead.

6.1.3 Scenario 1: Additional large consumers

The main finding in the results for this scenario is that the battery systems for the very large consumers spent all the time performing reserve market services. Their power consumption was so high that there were no capacity steps they could peak-shave under. By looking at the results page it is clear the more of the revenue came from the reserve markets. A very interesting observation is that even though the revenue increased dramatically in total, the revenue per kWh and kW is lower than the base case. This indicates that the smaller systems have better profitability when they are able to peak-shave, which also proves that providing multiple grid services increases profitability compared to single-service applications.

6.1.4 Scenario 2: C-rating change

When increasing the C-rating from 0.5 to 1.0, effectively doubling the power rating, the agents get more revenue from the reserve markets. Doubling the power rating doubles the power reserves that the battery system can provide to the reserve markets. As a result, the battery systems increased the reserve market participation and also increased revenue as a result. In general, the energy storage capacity is the main factor in battery costs. When the revenue almost doubles from the base case, a battery system developer should increase the power rating as much as possible as long as costs do not drastically increase.

Another interesting metric to evaluate is that the peak-shaving success rate went from 10% in the base case to 8% in this scenario. This shows that increasing the power rate did not increase the probability of peak-shaving successfully. The reason the peak-shaving success rate went down is probably because the possible available value that could be obtained on the reserve market was more attractive than the peak-shaving service. The trading on the local market also did not help specific agents in peak-shaving when needing to. This caused the capacity step for some agents to be broken.

6.1.5 Scenario 3: FFR removed

When deactivating the FFR market, the revenue reduced. This is to be expected since the FFR market is highly priced. The participation in all other services increased, but in most cases the agents decided to participate in the FCR D-2 market instead. The results in this scenario is closer to resembling the expected revenue for distributed batteries performing peak-shaving, reserve market participation and energy arbitrage.

6.1.6 Scenario 4: 2021 energy prices

When using the energy prices from 2021 the energy arbitrage revenue increased substantially from 1.8% to 15.9% of the total revenue. This service has now become a major contributor to the total revenue. This could indicate that if the energy prices remain at exceeded levels, the energy arbitrage service could have a significant role in increasing profitability of battery systems in the power grid. An interesting metric to observe is the total energy traded. The total traded reduced from 62.0MWh to 41.9MWh. This is due to how the optimization model was designed and to the characteristics of the energy prices. If the energy prices two days ahead are much higher than the prices one day ahead the agents will charge during the first day and sell the second day. This is often the case for the energy prices in 2021. In 2019 the energy prices varied during the day and the agents would therefor charge and sell the same day. This increases the total volume of energy traded. The price differences in 2021 were substantially higher than in 2019, so even with a lower volume traded, the revenues were substantially higher.

6.2 Model performance

The implemented model provides good results, but it is difficult to evaluate the performance since a fully optimal solution is too computational heavy to solve. The design choices is critically analyzed in this section.

6.2.1 Optimization

The optimization process was designed to be computationally efficient. The model achieved this very well. The run-time of the computational process was less than 1 microsecond for every agent, making the simulations run smoothly. The optimization process managed to present good results and performed as expected. There are two main design flaws in the optimization process.

Firstly, the method of determining the monthly capacity step for each agent is statistically inaccurate. The model used the compounding statistical probability of the power consumption being under a capacity step, assuming that the power consumption for each hour are independent events. While this method yielded decent results through testing, it is not a scientific approach. The power consumption for each hour are not independent events, and therefore the probability outputs does not give a realistic probability of what the needed capacity step should be. There are other approaches that could be utilized to yield a more accurate capacity step. For example: The model could look at the historical maximum monthly power consumption to provide an indication of future capacity steps. This can be done through calculating a moving average of past consumption or by analyzing the capacity steps of previous years, if the data exists. This would be a good approach for aggregated areas or businesses with continuous operation, but would not work well for businesses with sporadic and inconsistent power consumption. Again, a tool for personalized analysis could result in more accurate outcomes.

Secondly, the optimization relies too much on the forecasting error to determine the value of services. Battery systems with bad forecasting are more likely to spend more time on the peak-shaving service, which reduces profitability if there is actually no need for the peak-shaving service. A way to increase profitability is to let the agents with bad forecasting perform more reserve market services and instead use the local market for trading with other agents if the forecast deviates far from the expected power consumption.

The battery system and model has not been closely tuned to match the characteristics of the consumer. Aggregated areas have different consumption profile than commercial buildings. The aggregated area could need a higher energy capacity rather than a high power output. In other words; a high C-rating is not as important for aggregated areas than it is for commercial buildings with intensive power outputs. Personalizing the battery system to be optimally integrated with a power consumer will likely increase profitability.

There are some optimization design choices that are valuable contributions to the model. The choice of attributing a value to each service for each hour for each agent is a viable strategy for an easily scalable system. If every service a battery system can provide is attributed a value, it is trivial for the battery system to provide the service that yields the highest value. This strategy allows the model to include and exclude services depending on the wishes of the battery owner without needing to reprogram the model.

Chapter 7

Conclusion and future work

This thesis aimed to research agent-based control mechanisms for distributed BESS to provide energy arbitrage, peak-shaving and reserve market participation services. These services were chosen out of the identified BESS services provided in Table 2.1 to be optimal for the scope of this thesis. Based on simulations in a developed and implemented model, it can be concluded that agent-based models can be utilized to increase BESS flexibility and revenue. The results indicate that the developed model increases revenue when providing multiple services compared to single-service applications. The results also show that trading of service obligations between agents slightly increase revenue and increases the overall system flexibility. The implemented model proved to be a robust tool with simulation animation capabilities to analyze the response of the battery agents with changing scenarios.

The research in this thesis illustrates the ability of BESS being a provider of energy- and flexibility services, but also raises the question of the willingness and ability of energy markets to support distributed BESS as a supplier of energy- and flexibility services. The time and minimum power restrictions on market bids cause limitations on distributed BESS participation. Therefore, future studies could address the implications of changing market restrictions to accommodate distributed generation- and load units.

In this thesis a model is developed with a concept for how to enable distributed flexibility resources like energy storage systems to respond to flexibility incentive signals in a coordinated manner. Currently, the market mechanisms for local and central flexibility are not developed and mature. Future work should develop the market incentives to reflect the actual societal value of distributed power flexibility in order to fully benefit from the distributed control proposed here. Market mechanisms that could improve the functionality of distributed flexibility sources include:

- Instantaneous energy- and flexibility market trading, in contrary to the daily or monthly bidding windows which currently exist.

- A public trading platform for trading energy- and flexibility obligations, to relieve market participants from sub-optimally carrying out their obligations.
- No minimum power bid restrictions. You could essentially bid any amount of power.
- Create markets for different categories of flexibility. For example: Flexibility with fast response time of less than 1 second.

These market mechanisms would allow for a free market where evaluations for services are priced more correctly.

The model needs to be personalized to improve the forecasting method for specific users. In this thesis, consumers are assumed to have power consumption with clear trends. The Prophet forecasting algorithm was implemented in the model to easily detect underlying trends. Other consumers have trends that are not easy to detect for the Prophet algorithm. There are other forecasting methods that would work more optimally on those consumers. Since the optimization accuracy is highly dependant on the forecasting accuracy of the power consumption, personalizing the forecasting method to specific consumers could greatly increase profitability for the specific users.

The agent-based modeling proposed in this thesis for distributed battery systems for multiple grid services can be further developed for additional power flexibility sources, such as distributed loads like electric vehicle chargers, water heaters and generators such as wind- and solar power. An Internet of Things (IoT) platform could be developed to visualize and control the distributed units. The IoT platform could also be developed to optimize bids and autonomously deliver them to power market participants. A major advantage with creating an IoT platform with many generator and load units is that it circumvents the minimum bid restriction since the IoT platform can aggregate power from many distributed units.

Bibliography

[1] A. P. Sørdalen, 'Optimal integration and control of distributed batteries for multiple grid services,' *Unpublished work*, p. 42, 2021.

[2] RegjEV, *Norway is electric*, `https://www.regjeringen.no/en/topics/transport-and-communications/veg/faktaartikler-vei-og-ts/norway-is-electric`, Accessed: 2022-5-6, 2021.

[3] A. Gupta, S. R. Vaishya, M. Gupta and A. R. Abhyankar, 'Participation of battery energy storage technologies in co-optimized energy and reserve markets,' *IEEE*, vol. ? No. ? P. 6, 2020.

[4] E. F. Bødal, P. C. del Granado, H. Farahmand, M. Korpås, P. Olivella, I. Munné and P. Lloret, 'Challenges in distribution grid with high penetration of renewables,' *INVADE*, vol. 1, no. 1, p. 50, Jun. 2017.

[5] H. Pandžić, Y. Wang, T. Qiu, Y. Dvorkin and D. S. Kirschen, 'Near-optimal method for siting and sizing of distributed storage in a transmission network,' *IEEE TRANSACTIONS ON POWER SYSTEMS*, vol. 30, no. 5, p. 12, 2015.

[6] L. Gaillac, J. Castaneda, A.-A. Edris, D. Elizondo, C. Wilkins, C. Vartanian and D. Mendelsohn, 'Tehachapi wind energy storage project: Description of operational uses, system components, and testing plans,' *IEEE*, vol. 1, no. 1, p. 60, 2012.

[7] A. Kadri and K. Raahemifar, 'Is economic feasibility of bess energy price arbitrage jurisdiction dependent?' *IEEE*, vol. 1, no. 1, pp. 1024–1029, 2018.

[8] D. Krishnamurthy, C. Uckun, Z. Zhou, P. R. Thimmapuram and A. Botterud, 'Energy storage arbitrage under day-ahead and real-time price uncertainty,' *IEEE*, vol. 33, no. 1, p. 10, 2018.

[9] K. Chatchairungruang and S. Suwankawin, 'Peak-shaving of feed-in pv power for residential pvbattery system with added feedback-adjustment scheme,' *IEEE*, vol. 1, no. 1, p. 4, 2021.

[10] N. Padmanabhan, M. Ahmed and K. Bhattacharya, 'Battery energy storage systems in energy and reserve markets,' *IEEE TRANSACTIONS ON POWER SYSTEMS*, vol. 35, no. 1, p. 12, 2020.

[11] B. Gundogdu, D. T. Gladwin and D. A. Stone, 'Battery soc management strategy for enhanced frequency response and day-ahead energy scheduling of bess for energy arbitrage,' *IEEE*, vol. 1, no. 1, pp. 7635–7640, 2017.

[12] B. Xu, J. Zhao, T. Zheng, E. Litvinov and D. S. Kirschen, 'Factoring the cycle aging cost of batteries participating in electricity markets,' *IEEE TRANSACTIONS ON POWER SYSTEMS*, vol. 33, no. 2, p. 2, 2018.

[13] T. Morstyn, A. V. Savkin, B. Hredzak and V. G. Agelidis, 'Multi-agent sliding mode control for state of charge balancing between battery energy storage systems distributed in a dc microgrid,' *IEEE TRANSACTIONS ON SMART GRID*, vol. 9, no. 5, p. 9, Sep. 2018.

[14] R. J. Bessa, V. Miranda, A. Botterud, Z. Zhou and J. Wang, 'Time-adaptive quantile-copula for wind power probabilistic forecasting,' *Elsevier*, vol. 40, no. 1, p. 11, 2011.

[15] D. L. Feixiang Gong Ninghui Han and S. Tian, 'Trend analysis of building power consumption based on prophet algorithm,' *2020 Asia Energy and Electrical Engineering Symposium*, vol. 0, no. 0, p. 5, 2020.

[16] F. U. M. Ullah, A. Ullah, I. U. Haq, S. Rho and A. S. W. Baik, 'Short-term prediction of residential power energy consumption via cnn and multi-layer bi-directional lstm networks,' *IEEE*, vol. 8, no. 0, p. 12, 2019.

[17] Z. Li, K. Li, Z. Xuan, Z. Zhen and F. Wang, 'Decomposition-accumulation principle-based monthly electricity consumption forecasting approach using emd-xgboost hybrid model,' *IEEE*, vol. 1, no. 1, p. 6, 2019.

[18] Y. Yan and Z. Zhang, 'Cooling, heating and electrical load forecasting method for integrated energy system based on svr model,' *IEEE*, vol. 1, no. 1, p. 6, 2021.

[19] T. Dragicevic, X. Lu, J. C. Vasquez and J. M. Guerrero, 'Dc microgrids—part i: A review of control strategies and stabilization techniques,' *IEEE TRANSACTIONS ON POWER ELECTRONICS*, vol. 31, no. 7, pp. 4876–4891, Jul. 2016.

[20] J. Schönberger, R. Duke and S. D. Round, 'Dc-bus signaling: A distributed control strategy for a hybrid renewable nanogrid,' *IEEE TRANSACTIONS ON INDUSTRIAL ELECTRONICS*, vol. 53, no. 5, pp. 1453–1460, oct. 2006.

[21] I. V. Prasanna, D. Srinivasan and S. K. Panda, 'Design, analysis and implementation of a four-tier centralized control architecture for intelligent operation of grid-connected microgrids,' *IEEE TRANSACTIONS ON INDUSTRIAL ELECTRONICS*, vol. 1, no. 1, p. 6, 2016.

[22] C. Li, J. C. Vasquez and J. M. Guerrero, 'Multiagent-based distributed control for operation cost minimization of droop controlled dc microgrid using incremental cost consensus,' *IEEE*, vol. 1, no. 1, p. 4, 2015.

[23] H. Khani and M. R. D. Zadeh, 'Real-time optimal dispatch and economic viability of cryogenic energy storage exploiting arbitrage opportunities in an electricity market,' *IEEE*, vol. 6, no. 1, p. 11, 2015.

[24] R. H. Byrne, T. A. Nguyen, B. R. C. David A. Copp and I. Gyuk, 'Energy management and optimization methods for grid energy storage systems,' *IEEE*, vol. 6, no. 1, pp. 13 231–13 260, Aug. 2017.

[25] A. A. Thatte, L. Xie, D. E. Viassolo and S. Singh, 'Risk measure based robust bidding strategy for arbitrage using a wind farm and energy storage,' *IEEE*, vol. 4, no. 4, p. 9, 2013.

[26] C.-H. Yoo, I.-Y. Chung, H.-J. Lee and S.-S. Hong, 'Intelligent control of battery energy storage for multi-agent based microgrid energy management,' *MDPI*, vol. 6, no. 1, p. 24, 2013.

[27] X. Li and D. Zhang, 'Coordinated control and energy management strategies for hundred megawatt-level battery energy storage stations based on multi-agent theory,' *IEEE*, vol. 1, no. 1, p. 5, Aug. 2018.

[28] J. Lagorse, M. G. Simões and A. Miraoui, 'A multiagent fuzzy-logic-based energy management of hybrid systems,' *IEEE TRANSACTIONS ON INDUSTRY APPLICATIONS*, vol. 45, no. 6, p. 8, 2009.

[29] S. Abapour, B. Mohammadi-Ivatloo and M. T. Hagh, 'A bayesian game theoretic based bidding strategy for demand response aggregators in electricity markets,' *Sustainable Cities and Society 54*, vol. 1, no. 1, p. 8, 2020.

[30] *Powerwall*, Tesla, Oct. 2021.

[31] H. Nosair and F. Bouffard, 'Flexibility envelopes for power system operational planning,' *IEEE TRANSACTIONS ON SUSTAINABLE ENERGY*, vol. 6, no. 3, pp. 800–809, Jul. 2015.

[32] L. Lamport, *Advances in Renewable Energies and Power Technologies*, 1st ed. Amsterdam, 2018.

[33] S. Hochreiter and J. Schmidthuber, 'Long short-term memory,' vol. 1, no. 1, p. 33, 1997.

[34] R. Akter, J.-M. Lee and D.-S. Kim, 'Analysis and prediction of hourly energy consumption based on long short-term memory neural network,' *IEEE*, vol. 1, no. 1, p. 3, 2021.

[35] S. Luo, Y. Rao, J. Chen, H. Wang and Z. Wang, 'Short-term load forecasting model of distribution transformer based on cnn and lstm,' *IEEE*, vol. 1, no. 1, p. 4, 2020.

[36] S. J. Taylor and B. Letham, 'Forecasting at scale,' *PeerJPreprints*, vol. 1, no. 1, p. 25, 2017.

[37] T. Hastie and R. Tibshirani, 'Generalized additive models: Some applications,' *Journal of the American Statistical Association*, vol. 1, no. 1, pp. 371–386, 1987.

[38] Lede, *Pris på nettleie*, https://lede.no/pris-2022/category3109.html, Accessed: 2021-12-10, 2021.

[39] Elvia, *Nettleiepriser og effekttariff for bedrifter med årsforbruk over 100.000 kWh*, https://www.elvia.no/nettleie/alt-om-nettleiepriser/nettleiepriser-og-effekttariff-for-bedrifter-med-arsforbruk-over-100000-kwh/, Accessed: 2021-12-10, 2021.

[40] Statnett. 'Primærreserver - fcr.' (2021), [Online]. Available: https://www.statnett.no/en/for-stakeholders-in-the-power-industry/system-operation/the-power-market/reserve-markets/ (visited on 10/02/2022).

[41] Statnett. 'Primærreserver - fcr.' (2021), [Online]. Available: https://www.statnett.no/for-aktorer-i-kraftbransjen/systemansvaret/kraftmarkedet/reservemarkeder/primarreserver/.

[42] Regjeringen. 'Renewable energy production in norway.' (2016), [Online]. Available: https://www.regjeringen.no/en/topics/energy/renewable-energy/renewable-energy-production-in-norway/id2343462/.

[43] Statnett, *Demonstrasjonsprosjekt for Fast Frequency Reserves (FFR) 2021*, https://www.statnett.no/for-aktorer-i-kraftbransjen/systemansvaret/kraftmarkedet/reservemarkeder/ffr/ffrdemo2021/, Accessed: 2022-02-15, 2021.

[44] Z. Abdmouleh, A. Gastli, L. Ben-Brahim, M. Haouari and N. A. Al-Emadi, 'Review of optimization techniques applied for the integration of distributed generation from renewable energy sources,' *Renewable Energy 113*, vol. 1, no. 1, pp. 266–280, 2017.

[45] F. Lambert, *Tesla's massive Powerpack battery in Australia cost 66 million and already made up to 17 million*, https://electrek.co/2018/09/24/tesla-powerpack-battery-australia-cost-revenue/, Accessed: 2022-6-1, 2018.

NTNU

Norwegian University of
Science and Technology